# THE TAMILNADU DR. M.G.R. MEDICAL UNIVERSITY

# CHENNAI, TAMIL NADU.

## ASSESSMENT OF LONGITUDINAL STRAIN IN ACUTE ST-ELEVATION MYOCARDIAL INFARCTION

**DISSERTATION SUBMITTED FOR DM**

**(Branch II- Cardiology)**

**August-2011**

# CERTIFICATE

This is to certify that this dissertation titled "**ASSESSMENT OF LONGITUDINAL STRAIN IN ACUTE ST-ELEVATION MYOCARDIAL INFARCTION** " submitted by Dr.P.Ashok Kumar, to the faculty of Cardiology, The Tamilnadu Dr.M.G.R.Medical University, Chennai in partial fulfillment of the requirement for the award of DM degree Branch [Cardiology] is a bonafide research work carried out by him under our direct supervision and guidance.

*Professor and Head*
Department of Cardiology
Madurai Medical College and
Government Rajaji Hospital, Madurai

# DECLARATION

I, Dr.P.Ashok Kumar, solemnly declare that the dissertation titled “ASSESSMENT OF LONGITUDINAL STRAIN IN ACUTE ST-ELEVATION MYOCARDIAL INFARCTION ” has been prepared by me. This is submitted to The Tamilnadu Dr.M.G.R.Medical University, Chennai, in partial fulfillment of the regulations for the award of DM degree Branch [Cardiology].

Madurai. **Dr.P.Ashok Kumar**
Date:

## INTRODUCTION

Coronary Artery Disease is the leading cause of death worldwide. Every year about 100,000 people in the United States suffer acute Myocardial Infarction (AMI)[1]. The AMI incidence though shows declining trend in the west it is on the rise in the developing world. Effective management of this increasing epidemic imposes a technical challenge as well as a socio-economic burden to the third world countries. In addition to the routine clinical and Electrocardiographic (ECG) evaluation, Echocardiography is an integral part of AMI management. Assessment of overall Left ventricular (LV) function and the regional wall motion of individual myocardial segments is the essence of Echocardiography in the patients with AMI. Traditionally the regional wall motion is assessed subjectively by 2D imaging and objectively by calculation of wall motion score index. Global LV function is usually assessed by Teichzolts and Simpson`s methodologies. These modalities have their own limitations in patients with Acute myocardial infarction. Tissue Doppler imaging offsets some of the disadvantages of 2D echocardiography but by itself has several disadvantages in the assessment of regional and overall LV function. The introduction of Strain imaging has added substance to the imaging of patients with AMI. Strain and strain rate imaging has overcome the disadvantages of 2D as well as Tissue Doppler imaging and has stood the test of time since its introduction a decade ago. The modality of Strain imaging is fast advancing with the initial reports of Doppler based strain imaging now giving way to strain by 2D Speckle tracking.

This study utilizes Longitudinal strain derived by 2D speckle tracking for assessment of regional and global LV function in patients with AMI and compares the same with traditional parameters like Wall motion score index and 2D derived Ejection Fraction (EF).

## REVIEW OF LITERATURE

The usual indices of global left ventricular (LV) function, such as ejection fraction and volumes, are load-dependent, and standard volumetric approaches to their measurement may be influenced by image quality, technical considerations such as off-axis imaging, and measurement error. The assessment of regional function is more difficult, remains highly subjective, and requires significant training.[2]

**Regional Wall Motion Analysis:**

The immediate manifestation of myocardial ischemia is a decrease in or cessation of myocardial contractility (systolic thickening), even before the occurrence of ST-segment changes or the development of symptoms. Ischemic myocardium may continue to demonstrate some degree of passive forward motion because of the pulling action of adjacent nonischemic muscle, but the contractility (systolic thickening) of the ischemic myocardial segments is decreased (hypokinesis) or absent (akinesis). Normally, left ventricular (LV) free wall thickness increases more than 40% during systole. In normal subjects, the percentage of thickening of the ventricular septum is somewhat less than that of the free wall of the LV. Hypokinesis is defined as systolic wall thickening less than 30%, and akinesis is defined as wall thickening less than 10%. Dyskinesis is defined as a myocardial segment moving outward during systole, usually in association with systolic wall thinning.

With multiple tomographic imaging planes, two-dimensional (2D) echocardiography allows visualization of all LV wall segments. For purposes of regional wall motion analysis, the LV is divided into several segments. The American Society of Echocardiography has recommended a 16-segment model [3] Optionally, the apical tip is added as a 17th segment. Each segment is

assigned a score on the basis of its contractility as assessed visually: normal = 1, hypokinesis = 2, akinesis = 3, dyskinesis = 4, and aneurysm = 5.(Table 1) On the basis of this wall motion analysis scheme, a wall motion score index (WMSI) is calculated to semiquantitate the extent of regional wall motion abnormalities:

WMSI= sum of wall motion scores/ Number of segments visualized

A normally contracting LV has a WMSI of 1 (each of the 16 segments receives a wall motion score of 1; hence, the total score is 16 and WMSI is 16/16 = 1). The larger the infarct the higher the WMSI because wall motion abnormalities become more severe.

| WALL MOTION SCORE | Score |
|---|---|
| Normal | 1 |
| Hypokinesia | 2 |
| Akinesia | 3 |
| Dyskinesia | 4 |
| Akinesia | 5 |

Table 1: Table showing standard wall motion scores. Optional scores include 0 for hyperdynamic myocardium, 6 for Akynesia with scar, 7 Dyskinesia with scar.(Not included in this study)

What does the WMSI indicate? Because the echocardiographic analysis of wall motion abnormality is subjective and the reduction of systolic myocardial thickening is not proportional to the incremental amount of infarcted or ischemic myocardial tissue [4], the correlation of the WMSI with the actual size of the myocardial infarct or the perfusion defect may not be good in the case of acute myocardial infarction. When a 2D echocardiographic examination was performed simultaneously with an injection of sestamibi in patients with acute myocardial

infarction with ST-segment elevation on the ECG, the overall correlation between the WMSI and the perfusion defect was good [5]. Patients with WMSI greater than 1.7 had a perfusion defect larger than 20%. The correlation was better in patients with an anterior wall myocardial infarction than in those with an inferior or lateral wall myocardial infarction with a smaller infarct size. However, it is possible to have relatively normal myocardial contractility when there is a myocardial perfusion defect. Also, the reverse is true, depending on the clinical situation. Without a previous ischemic insult, a small subendocardial perfusion can be present when no visible contractility abnormality is evident. However, the myocardium may remain akinetic for a period of time after coronary reperfusion. Therefore, knowledge of both myocardial contractility and perfusion is vital for the management of the subset of patients with coronary artery disease. Another interesting subset of patients with acute myocardial infarction is the group with normal coronary arteries, for example, patients with apical ballooning syndrome, subarachnoid hemorrhage, or pheochromocytoma or those who have had electroconvulsive therapy. In these situations, marked wall motion abnormalities are present acutely but perfusion is normal. These wall motion abnormalities usually resolve in 5 to 10 days.

**Technical Caveats**

A reliable regional wall motion analysis is among the most challenging tasks in echocardiography. All available windows and tomographic planes should be used to visualize all the LV segments. Apical short- and long-axis views are especially useful in evaluating the apical third of the LV. Continuous scanning from the apical four-chamber to the apical long-axis to the apical two-chamber view allows complete visualization of all LV segments. In patients who have

chronic obstructive pulmonary disease or who are obese, a lower frequency (2.0-2.5 MHz) transducer should be used to optimize the definition of the endocardium, and the subcostal window may provide adequate visualization of the LV segments. A new imaging method that uses the principle of harmonic resonance (native harmonic imaging) can improve visualization of the endocardium. In patients with a good apical window, the use of higher frequency transducers, with adjustment of the focal zone to the near region, may enhance the definition of the apical endocardium, help delineate apical wall motion abnormalities, and differentiate thrombus from apical trabeculation.[6]

The assessment of regional wall motion on echocardiography is limited when visualization of the LV endocardium is not adequate. Several new modalities may enhance the ability to analyze regional wall motion.

**Global Left Ventricular Function assessment by Ejection Fraction**

The most popular expression of global LV function is the LVEF. LVEF is a simple measure of how much of the end-diastolic volume is ejected or pumped out of the LV with each contraction. Although readily influenced by loading conditions, this simple measure has been found to be a strong predictor of clinical outcome in almost all major cardiac conditions and is used to select the optimal management strategy, including the implantation of an intracardiac defibrillator or biventricular pacing [7,8]. Most frequently, LVEF is determined visually by eyeballing 2D echocardiographic images of the LV. This visual assessment is reasonably reliable when performed by an experienced echocardiographer but has considerable interobserver variation[7]. Therefore, whenever possible, the LVEF should be measured more objectively by using

volumetric measurements. Quantitatively, LVEF can be calculated from M-mode, 2D, and 3D echocardiograms.

M-mode recording of 2D measurements of LV dimensions from the mid ventricular papillary muscle level is used to calculate the LVEF as follows,[9]

$$LVEF = (\%D^2) + (1 - D^2)(\%L)$$

$$D^2 = LVDE^2 - LVES^2 / LVED^2 \times 100$$

where %Î”$D^2$ is the percentage fractional shortening of the square of the minor axis, and %Î”L is the percentage fractional shortening of the long axis, mainly related to apical contraction: 15% for normal, 5% for hypokinetic apex, 0% for akinetic apex, -5% for dyskinetic apex, and -10% for apical aneurysm.

There are two components in the equation. The first component is actually a percentage change in the LV area or fractional shortening of the square of the LV short axis. If it is assumed that the apical long-axis dimension remains the same during systolic contraction, the percentage area change or fractional area change is equal to the percentage volume change. Because the apical long axis shortens 10% to 15% with systole, an apical correction factor, the second component, is added. This factor varies with the contractility of the apex.

LVEF is perferrably calculated from 2D or 3D volume measurements. Although there are several different methods for measuring LV volume and LVEF from 2D echocardiographic images of the LV, the disk summation or biplane Simpson method is used most often. The LV endocardial border is traced from one apical or two orthogonal apical views to create multiple (usually 20) cylinders whose volume is summated to provide LV volume. It is most critical to trace the actual endocardial border, not the trabeculations. Trabeculations and papillary muscles should be

included as a part of the LV cavity, not as part of the LV wall. If the definition of the endocardial border is not clear, the intravenous administration of a perfluorocarbon contrast agent will help delineate this border. LV volume is usually larger when measured with the contrast agent.

Another crucial technical point for reliably measuring LV volume is avoiding foreshortening of apical views. The apical long axis is divided by the number of cylinders created within the LV, and the resulting distance (long-axis dimension Ã· number of cylinders) becomes the height of each cylinder. Therefore, the long-axis dimensions from two apical views should be similar. In subjects with uniform contractility, LV volume measured with a single plane is very close to the LV volume obtained with the biplane Simpson method. The biplane Simpson method is preferred for measuring the L volume of an LV with regional wall motion abnormalities. In any given view, a circular disk is assumed at each level along the ventricle. Obviously, if a regional wall motion abnormality is not visualized in the plane of examination, this technique will overestimate the ejection fraction. For this reason, when dealing with patients with coronary disease in whom regional abnormalities are anticipated, biplane methodology is necessary if precise measurements are required. Because of the regional nature of coronary disease, other methods, such as area length calculations, have had less acceptance in evaluating patients with coronary disease.[10]

The echocardiographic measurement of myocardial strain (€) offers a series of regional and global parameters that may be useful in the assessment of systolic and diastolic function. Strain is a measure of tissue deformation. As the ventricle contracts, muscle shortens in the longitudinal and circumferential dimensions (a negative strain) and thickens or lengthens in the radial direction (a positive strain)[2]. The application of strain to measure deformation is

constrained by a number of complexities when the parameter is measured by echocardiography. First, to quantify the lengthening or shortening process an initial measurement of length is required (Lagrangian strain), and the same findings may not necessarily be obtained by the measurement of instantaneous strain during contraction (Eulerian or natural strain). Second, tissue deformation occurs in three planes, in addition to which shearing motion involves a number of other tensors, so our current measurement approaches are a vast simplification of the true motion of the heart. Third, the assumption that tissue is incompressible is not completely true, and for example ignores the variation in myocardial blood volume between diastole and systole. Fourth, the complexities of fiber direction cause a longitudinal shortening of 20% to 30% to generate radial shortening of 50% to 70% [11]

Myocardial strain may be measured using a variety of echocardiographic techniques. Although M-mode techniques provide both accurate temporal and accurate spatial resolution, and may therefore be used to measure strain in a single dimension, the current era of myocardial strain measurement began with the measurement of SR from comparison of adjacent tissue velocities by Heimdal et al. [12] Subsequently, strain has been measured using speckle tracking techniques [13] Each of these methodologies presents its own clinical challenges.

**Tissue Doppler-based strain.**

**TECHNICAL ASPECTS**. The velocity of movement of myocardium can be recorded by tissue Doppler techniques and displayed as a parametric color image in which each pixel represents the velocity relative to the transducer. These data may also be expressed graphically as the velocity of the myocardium relative to time (on the x axis). These recordings have documented

that a descending gradation of velocity exists from the LV base to apex, reflecting the contraction of the base toward a relatively fixed apex. There is a gradation of peak velocities at different locations along the LV wall. Although these velocity recordings provide information about the motion of the wall, the ability of contraction in adjacent segments to influence the velocity in any given segment limits the site-specificity of velocity data. Rather than examine the motion of a segment relative to the transducer, which is susceptible to tethering to adjacent tissue, myocardial motion may be measured relative to the adjacent myocardium. The instantaneous gradient of velocity along a sample length may be quantified by performing a regression calculation between the velocity data from adjacent sites along the scan line, and these instantaneous data may then be combined to generate an SR curve[14]. Integration of this curve provides instantaneous data on deformation—shortening or lengthening—that represent strain (Fig. 1). These data therefore reflect the movement of one tissue site relative to another within the sample volume, in contrast to tissue velocity data, which merely reflect movement of one site relative to the transducer. A number of experimental and clinical articles have attested to the benefits of site specificity in avoiding motion caused by tethering to adjacent segments, which is especially important when dealing with coronary artery disease. [15,16] Like tissue velocity, strain parameters are most commonly used to assess myocardial motion in a base-to-apex direction, which is sensitive to mild subendocardial damage. In contrast, the measurement for radial strain from tissue velocity data is unsuitable for clinical use. It is difficult to accommodate the optimal inter-site distance required for SR measurements (12 mm) in a ventricle of normal thickness, and the use of a shorter offset distance is associated with greater noise levels. Moreover, the requirement for the adjacent points to lie along a single regression

line means that only anteroseptal and posterior segments can be analyzed with this technique, and because of the combination of right ventricular (RV) and LV myocardial structure in the septum, effectively only radial strain of the posterior wall measurements are meaningful.

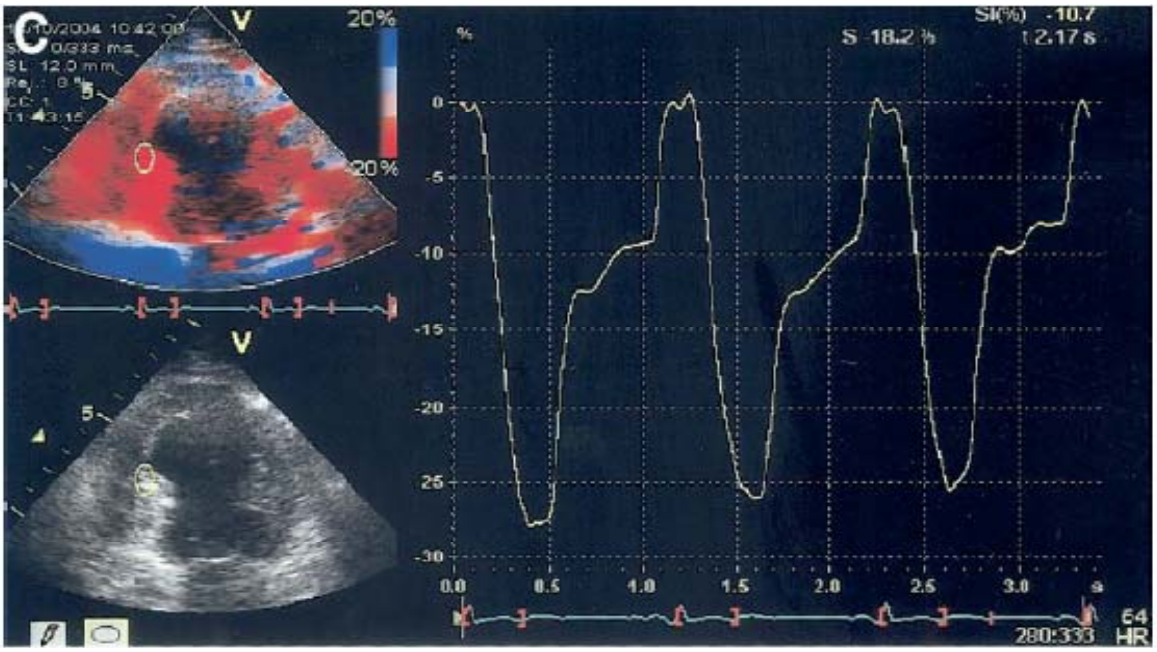


*Fig 1: Derivation of strain from tissue Doppler data. Regression calculation between adjacent tissue velocity data points along this length generates the strain rate curve, which is then integrated to calculate strain.*

**LIMITATIONS OF DERIVATION OF SR FROM TISSUE VELOCITY.**

The velocity-regression technique has a number of potential pitfalls (Table 2). First, the comparison of adjacent velocities is exquisitely sensitive to signal noise, and the quality of SR curves may vary depending on the care used in obtaining the underlying velocity data. Optimizing the velocity signal should include avoidance of reverberation artifact and ensuring adequate frame rate (100 frames/s). Inadequate pulse-repetition frequency leads to aliasing. Improvements to the velocity signal by use of harmonic imaging as well as both temporal and

spatial averaging are important in optimizing the SR signal, although this comes at the cost of reducing spatial resolution. The second limitation relates to the limits on spatial resolution that are imposed by imaging at high temporal resolution. If the number of Doppler interrogating beams is limited in an effort to maximize temporal resolution, spatial resolution may be compromised. This may contaminate myocardial velocity signals with adjacent LV blood pool velocities, which are an important source of noise. In turn, this will compromise the SR signal. Tracking the sample throughout the cardiac cycle is also important to ensure that the sample remains within the myocardium. Use of a narrow imaging sector—although inconvenient for clinical imaging— enables a limited number of Doppler beams to be focused in a small area, optimizing spatial resolution.

Table2: Problems and Solutions for Tissue-Velocity Based Strain Rate Imaging

| **Problem** | **Solution** |
|---|---|
| Signal noise | Ensure clean velocity signal (avoid reverberations on two-dimensional echocardiography)<br>Use harmonic imaging<br>Avoid aliasing on TVI signal (use adequate pulse repetition)<br>Track sample volume to left ventricular wall to avoid cavity signal |
| Underestimation | Use high frame rate |
| Angle dependence | Align axis of movement with scan line narrow sector |
| Through-plane motion | Caution with interpretation of events late after QRS |
| Respiratory drift | Acquire in end-expiration |

If a narrow sector is undesirable, reduction of frame rate will allow the use of more Doppler beams across the imaging sector, effectively sacrificing temporal for spatial resolution. These limitations on lateral resolution significantly limit the ability of the technique to assess longitudinal subendocardial and subepicardial SR during standard imaging.

Third, like all Doppler techniques, tissue velocity-based strain is sensitive to alignment. The application of this technique to areas where the axis of contraction changes along the scan line (e.g., the apex) means that different vectors may be involved at each site (Fig. 2), with consequent error in strain measurement [17]

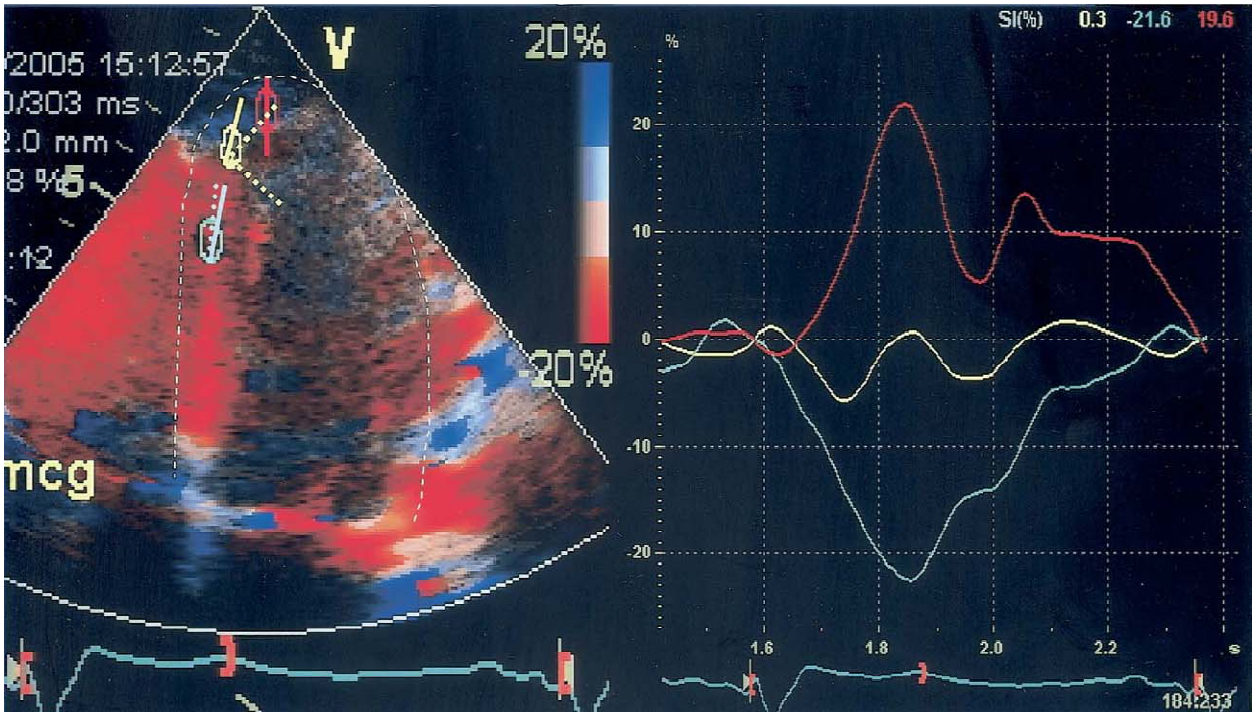


*Fig 2: Impact of angulations on strain rate imaging. Interrogation parallel with the wall (mid-septum, shown in blue) identifies long-axis shortening, and at right angles to the wall (apex, shown in red) identifies short-axis thickening. However, an intermediate angle (apical septum, shown in yellow) causes underestimation—a mixture of vectors at 45% produces a net absence of recordable strain. Scan planes are shown as continuous lines, longitudinal and radial contraction vectors as broken lines.*

Fourth, the derivation of data along the scan line means that the velocity regression technique is unidirectional. Even when tracking is used to try to maintain the sample volume within a segment of myocardium, it needs to be remembered that the myocardium undergoes a wringing, torsional motion so that the sample will inevitably move out of the scanning field in the course of the cardiac cycle. This motion has little effect on systolic measurements, because peak SR occurs early in systole, but it may become important in the measurement of diastolic phenomena. These considerations of through-plane motion may be particularly important when the myocardial function is non-uniform, as for example, with an ischemic cardiomyopathy. Finally, angle changes during the cardiac cycle and with respiratory movement may contribute to drifting of the strain curve. These technical challenges of tissue velocity based SR measurements can be avoided by careful acquisition or by the use of speckle derived measurements.

**VALIDATION.** Despite these limitations, it is important to acknowledge that this technique has been extensively validated, initially with sonomicrometry [18] Subsequent studies have confirmed correlation with magnetic resonance imaging [19]

**Echocardiography-based measurement of strain.**

**RATIONALE** A Doppler-independent technique for strain measurement would have attractions with respect to signal noise, angle dependency, and the ability to monitor strain in two dimensions rather than one dimension. Various echocardiographic techniques have been used, including comparison of adjacent radiofrequency signals, and more recently, block-matching and speckle tracking techniques [20,21] These **speckles are ultrasound reflectors within tissue, are highly reproducible, and essentially behave like magnetic resonance tags** (Fig. 3). Shortening

may be calculated by comparison of these speckles from frame to frame, although attention to technical detail is important, because comparisons at high frame rates are associated with high levels of noise, and comparisons at low frame rates risk loss of correlation because of excessive displacement of the speckles.

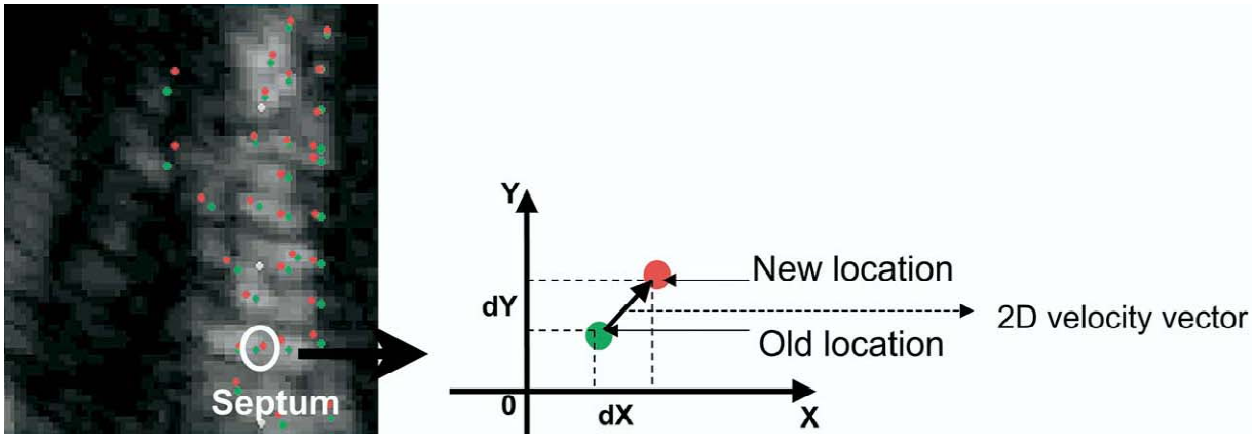


*Fig 3: Two-dimensional (2D) strain is based on comparison of the image texture (i.e., pattern of individual speckle elements) from frame to frame. The distortion of this pattern permits assessment of strain in the axis of movement rather than the axis of the ultrasound beam.*

**COMPARISON WITH TISSUE VELOCITY METHODOLOGY.** Because the assessment incorporates baseline length, twodimensional (2D) strain (in contrast to the velocity regression approach) is able to measure Lagrangian strain. The approach also has the added attraction of offering a feasible approach to radial measurements, which may be a more accurate measure of wall thickening than M-mode echocardiography, in which a proportion of apparent thickening is thought to reflect joining of the trabeculae. Finally, the technique offers a completely new approach to the assessment of torsional motion, derived from circumferential strain at different levels in the heart. However, differences in frame rate and smoothing lead to the availability of less detail in the SR and strain curves, with potential difficulties in the

measurement of timing parameters.(Table 3) Nonetheless, magnitude parameters seem to be analogous with the 2D strain and velocity regression approaches [20]

*Table 3: Parameters Obtained From Strain Rate Imaging*

| Type of Parameter | Specific Measurement | Comment |
|---|---|---|
| Timing | Time to onset of systole and time to relaxation | Problems with reproducibility in clinical settings, may be less suited to 2D strain due to lower temporal resolution. |
| Magnitude (longitudinal or radial) | Peak systolic strain rate | Susceptible to angulation issues with TVI-based strain, probably more robust with 2D strain but frame rate may be a limitation |
| | Peak diastolic strain rate | Through-plane motion may limit site specificity. |
| | Peak systolic strain | Corresponds with regional ejection fraction and may be less suited to stress echocardiography |
| Magnitude + timing | End-systolic strain | Dependent on accurate defining of end-systole, lacks information about rate of contraction. |
| | Post-systolic thickening | Not a specific marker of ischemia. |

**COMPARISON WITH TISSUE VELOCITY METHODOLOGY.** Because the assessment incorporates baseline length, twodimensional (2D) strain (in contrast to the velocity regression approach) is able to measure Lagrangian strain. The approach also has the added attraction of offering a feasible approach to radial measurements, which may be a more accurate measure of wall thickening than M-mode echocardiography, in which a proportion of apparent thickening is thought to reflect joining of the trabeculae. Finally, the technique offers a completely new approach to the assessment of torsional motion, derived from circumferential strain at

different levels in the heart [22] However, differences in frame rate and smoothing lead to the availability of less detail in the SR and strain curves, with potential difficulties in the measurement of timing parameters. Nonetheless, magnitude parameters seem to be analogous with the 2D strain and velocity regression approaches, ischemic myocardium, but although delayed contraction is a pathophysiological hallmark of ischemia, and despite some favorable clinical results[23], the clinical application of timing parameters is limited by measurement variations. It seems more feasible to obtain these results using tissue velocity signals, which, although not site-specific, are less prone to artifact.

**MAGNITUDE PARAMETERS:** Normal ranges of SR and strain have been described [24] Normal resting values for longitudinal SR vary between 1.0/s and 1.4/s, with the standard deviation in most locations ranging from 0.5/s to 0.6/s. Normal longitudinal systolic strain in most segments varies from 15% to 25%, with normal radial strains ranging from 50% to 70%, and standard deviations of 5% to 7%. Although reproducibility data have been published, there has been little attention to test/retest variation, which is important if the technique is to be used in serial follow-up. Normal ranges for magnitude parameters are influenced by increasing age, pre-load (strain increases as LV size increases), and after-load (strain decreases with increasing blood pressure). Strain rate seems to be less dependent on loading. Regional variations pose an even greater problem—in addition to ischemia, these may be caused by curvature or by non-uniform fiber direction and differences in angulation. The magnitude parameters obtained by Tissue Doppler strain correlates well with Speckle derived strain.[25]

**DATA ACQUSITION**: Although integration of a regional velocity curve measures regional displacement, the integration of a regional SR curve will derive the regional curve (Figure 4).

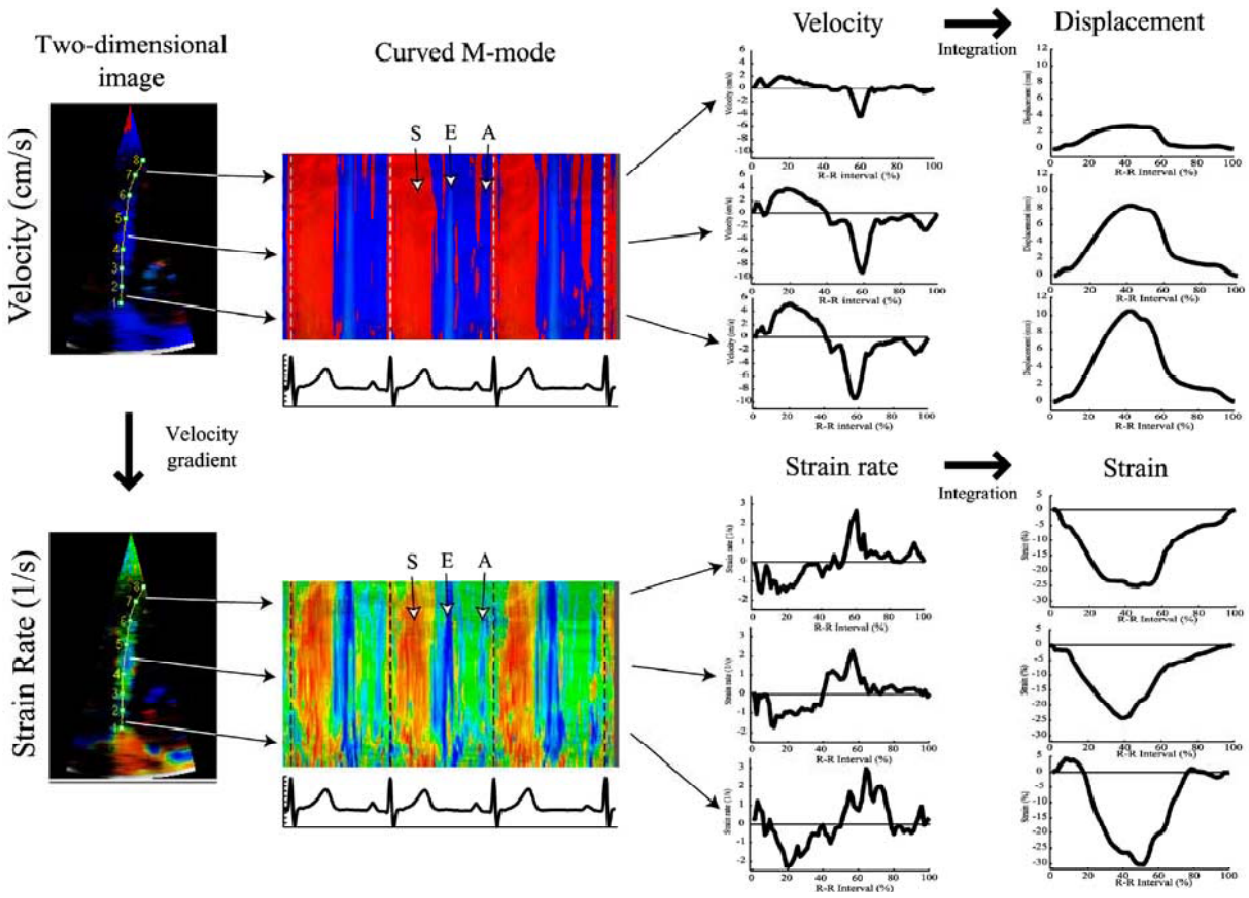


*Fig 4: Data sets derived from high frame rate 2-dimensional (2D) color Doppler myocardial velocity can be displayed either as real-time 2D velocity (top left) or strain rate (SR) (bottom left) image. Regional velocity or SR profiles can also be derived from any selected point in 2D data sets during postprocessing*

Although regional systolic strain rates (SRs) measure the rate of local deformation, regional systolic strain expresses the percentage of deformation (note that regional estimation provides no information on absolute wall thickness but only measures relative changes). Each regional strain curve can be subdivided into component parts, each of which represents a different mechanic phase of cardiac cycle (Figure 5). This subdivision is done by incorporating timing data for global mechanical events into the SR/strain curve. Normally, such subdivision of the SR/strain curve is on the basis of determining the timing of aortic valve opening, aortic valve

closure, and mitral valve opening. Currently, radial strain can only be processed reliably for

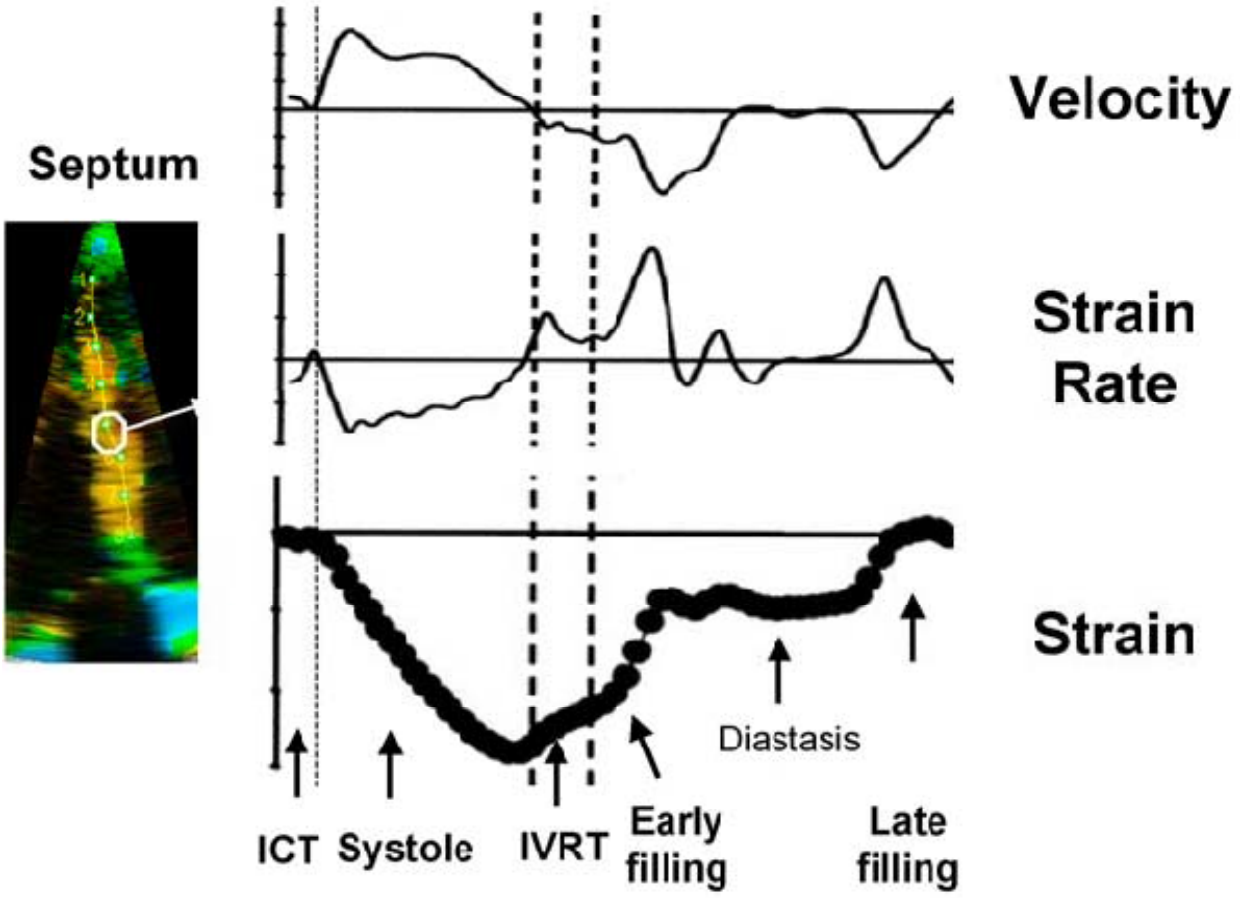


*Fig 5: Data on timing of global events is implanted into normal regional velocity, strain rate, and strain rate (SR) curves to subdivide cardiac cycle into mechanical components. ICT, Isovolumic contraction time; IVRT, isovolumic relaxation time.*

posterior wall segments. Radial strain cannot be measured in the septum by current methods. This is most likely a result of the functionally bilayered structure of the interventricular septum and the presence of two radial velocity gradients within the septum, one on the left ventricular (LV) side and one on the right.

Normal segmental velocity, SR, and strain values for both radial and longitudinal function for a group of healthy adults (age 20-40 year) have already been defined by Sun JP et al as well as Kowalski et al.[24] In control subjects, peak systolic strain in the LV free wall segments is

significantly higher in the radial direction (normal radial peak systolic strain value: 50%-70%) compared with longitudinal peak systolic strain (normal value: 20%-30%) in the same segment. For each wall, the regional deformation curves can be time aligned and displayed together with the timing of global events to allow the evaluation of the temporal changes in regional deformation within the wall. In addition to recording regional radial and longitudinal SR/strain, it is also possible to resolve circumferential-radial shear strain. This describes the local torsion and twisting/untwisting, and can be derived from a series of parasternal short-axis views taken at apical and midpapillary muscle levels with data taken at high frame rate, ie, 200 frames/s.

**CHANGES IN PRELOAD, AFTERLOAD, and CONTRACTILITY: HOW DO THEY AFFECT SR MEASUREMENT ?**

Myocardial deformation is the result of the complex interaction of intrinsic contractile force and extrinsic loading conditions applied to a tissue with variable elastic properties. Therefore, changes in preload and afterload, and the changes in myocardial stiffness, are important determinants of the pattern and the magnitude of myocardial deformation. Thus, SR and strain indices are not direct measures of contractility. Mathematic modelling studies would predict that peak systolic strain values will increase with increasing preload as long as contractile function is preserved, [26] whereas peak systolic strain values will decrease both with increasing ventricular size and with increasing afterload (again with preservation of contractile function). Regional peak systolic values will also decrease if intrinsic contractility is reduced, as in regional ischemia or in cardiomyopathies. It is interesting to note that longitudinal end-systolic strain values should be proportionally more decreased by dilatation when compared with radial values. Changes in regional peak systolic SR may be more complex as this parameter is more

related to local contractile function and is less dependent on changes in preload or afterload. Indeed, **by measuring peak systolic SR (or, even better, rate of increase of SR) we may come closest in clinical practice to representing regional contractile function**. These modelling predictions have subsequently been substantiated in the experimental setting by Weidemann et al,[27] who studied normal myocardium. In this study, ultrasound-derived peak systolic SR correlated best with dP/dt (an index of contrac- tile function), whereas peak systolic strain correlated best with changes in stroke volume and, therefore, was more closely related to changes in global hemodynamics than changes in contractility.

## POTENTIAL CLINICAL APPLICATION OF STARIN IMAGING

### Ischemic Heart Disease

Despite several attempts to implement new cardiac ultrasound methods to quantify ischemia, the routine clinical evaluation of regional function in ischemic heart disease has remained firmly on the basis of visual assessment of wall motion and wall thickening. However, the eye has been shown to have limitations in assessing the timing of the complex changes in regional myocardial deformation that occur in differing ischemic substrates. Kvitting et al[28] showed that healthy individuals can neither reliably visualize nor time regional mechanical events when they occur at a time interval of less than 90 milliseconds. Thus, postsystolic thickening (PST), which is an important parameter to measure when attempting to quantify regional ischemia (and which usually lasts only 50-60 milliseconds), may neither be displayed by ultrasound systems with low frame rates nor, if displayed, be appreciated visually. Even in ultrasound systems with sufficiently high frame rates, it would be necessary to time aortic valve closure to determine the relative amounts of regional thickening/shortening that occur during or after ejection. Thus,

there is a need for a fully quantitative temporally resolved ultrasound approach to study the regional changes in deformation induced by ischemia. In theory, this approach could be on the basis of the high spatial and temporal resolution inherent in M-mode echocardiography. However, this approach often can only be applied to the quantification of radial function in two myocardial segments (basal septum and basal posterior wall). Long-axis function of each of the 4 cardiac walls can also be studied by M-mode by measuring atrioventricular plane displacement. However, this measurement only reflects the sum of the regional displacements in the underlying wall segments and does not, per se, measure regional function. **SR/strain imaging could, allow the quantification of longitudinal segmental deformation throughout a myocardial wall.** However, in the radial direction, it can normally only be applied to the posterior wall mid and basal segments. Several experimental studies have already shown that both radial and longitudinal 1-dimensional ultrasonic deformation indices can discriminate between the different ischemic substrates.[29] Such differentiation is on the basis of the comparison of regional deformation information acquired both at rest and during a low-dose dobutamine challenge. The sequence of changes in deformation consistently induced by acute ischemia has been well defined by both experimental sonomicrometric and cardiac ultrasound studies.[30,31] Acute ischemia induces both early systolic thinning and a delay in the onset of systolic thickening. There is also a flow related progressive decrease in the rate and degree of systolic thickening. Concomitant with the decrease in maximal systolic thickening, an abnormal ischemia-related thickening of the myocardium occurs after aortic valve closure. This abnormal phenomenon has been termed “ischemia-induced PST”. Experimental ultrasound studies have confirmed that with increasing severity of acute ischemia, there is a progressive reduction in

maximal systolic SR/strain with a concomitant development of increasing PST. Ischemia-related changes in systolic SR/strain indices have also been shown to be detectable earlier than are changes in either tissue velocities or the visual detection of regional wall-motion abnormalities. Stunned myocardium (ie, postischemic myocardium with flow reserve) has an abnormal deformation pattern at rest that is similar to that of ischemic myocardium (ie, myocardium with inadequate flow reserve). However, during a low-dose (10-15 mcg/kg/min) dobutamine challenge, the response of stunned versus ischemic myocardium was completely different. A "stunning" response is characterized by normalization of peak systolic SR/strain with an associated progressive decrease in PST, whereas an ischemic response is characterized by a dose-dependent increase in PST associated with either a reduction or no change in systolic SR/strain[32] Infarcted myocardium also has abnormal systolic and early diastolic deformation properties. The differentiation of an acute or chronic transmural infarction from a nontransmural infarction can also be achieved by combining a baseline study with a low-dose dobutamine challenge. A partial-thickness infarct will have markedly reduced systolic strain at rest (with some PST). During a low-dose dobutamine challenge a partial-thickness infarct will exhibit an ischemic response, ie, an increase in PST associated with a reduction or no change in systolic SR/strain. It has also been demonstrated that the deformation properties of a nontransmural infarct segment are closely related to the transmural extension of the scar; ie, the lower the systolic deformation the greater the transmural extension of scar in the region at risk. Conversely, transmural infarction is characterized by either no measurable systolic deformation or the presence of abnormal thinning/lengthening at rest, with no inducible increase in thickening/ shortening during a dobutamine challenge. The new ultrasound-based

deformation indices have also been used in the experimental setting to quantify changes in regional deformation induced by reperfusion injury. After the induction of an acute transmural myocardial infarction, acute reperfusion with Thrombolysis in Myocardial Infarction grade 3 (TIMI 3) flow induces an immediate marked and persistent increase in wall thickness, whereas the severely reduced peak systolic SR/strain and PST remain unchanged during reperfusion. It is interesting to note that in this study, during the progression of acute ischemia to transmural infarction, regional peak systolic SR decreased progressively to near 0 whereas the degree of PST was almost unchanged. PST also persisted during infarct reperfusion, showing that in transmural infarction, regional PST is a passive phenomenon and not a direct marker of segmental viability. Identical changes in deformation have also been observed for patients after primary coronary intervention (PCI) for acute infarction in whom TIMI 3 flow was re-established. Initial clinical studies have also confirmed that consistent changes in regional deformation are induced by vessel occlusion during PCI. In segments at risk (ie, those not supplied by collaterals) there is an immediate decrease in systolic SR/strain by some 50% compared with the baseline values. This is paralleled by the acute development of PST in the segment at risk during balloon inflation with no measurable change in deformation in distal nonischemic segments. On the other hand, in segments at risk supplied by collaterals balloon occlusion resulted in only minor changes in systolic SR/strain and less PST compared with noncollateralized segments at risk, indicating the protective nature of the collateral supply. In the same clinical setting, myocardial peak systolic velocities were unable to differentiate between collateralized and noncollateralized segments at risk. For each of the ischemic

substrates, the typical resting abnormalities and the changes induced by a low-dose dobutamine infusion are set out in.[33]

**Other Areas of potential use of Strain imaging:**

**The Quantification of Dobutamine Stress Echocardiography**

The visual assessment of regional myocardial function during dobutamine stress echocardiography (DSE) has been shown to be highly subjective and dependent on both image quality and experience. There is also a considerable difference in the interpretation of DSE among experienced readers. The visual inspection of stress echocardiography images is on the basis of the analysis of radial motion/thickening. However, ischemic changes first affect long-axis function. Because of this, a quantitative technique that assesses both radial and longitudinal function could enhance the clinical use and reproducibility of stress echocardiography. Initial attempts to use DMI to quantify stress echocardiography images have been on the basis of peak systolic velocity measurement. Although initial results have been promising, peak systolic velocity measurement could only be applied with confidence to the analysis of basal and midwall segments. Velocity measurement is also limited by both the confounding effect of the exaggerated translational motion of the heart during a stress test and the tethering that occurs between normal contracting and hypocontractile segments. Thus, subtle changes in regional contractility during DSE potentially should be better described by the measurement of local myocardial deformation indices. A series of clinical studies have shown that whereas regional SR/strain data acquisition is feasible during a standard DSE,[34] this approach is not practical during either treadmill or bicycle exercise, as these two latter stress modalities increase signal noise and, thus, preclude SR/strain measurement. During DSE studies

in control subjects, the findings of prior experimental studies were duplicated (ie, for normal myocardium, an incremental dobutamine infusion produces a linear segmental peak systolic SR response and a biphasic peak systolic _ response). In addition, the differing responses in deformation of ischemic, stunned, partial-thickness, and fullthickness infarcted myocardium to an incremental dobutamine challenge shown in experimental studies have all been reproduced in the clinical setting. Furthermore, Voigt et al, [35] in a correlative study comparing deformation changes induced during stress echocardiography with angiographic and perfusion scintigraphy data, showed that deformation could be quantified in 85% of segments and visual assessment of changes in curved M-mode SR curves could be evaluated in 95% of all segments. The ratio of induced postsystolic shortening to systolic shortening was found to be the best quantitative parameter with which to identify stress-induced ischemia, being 86% sensitive and 90% specific. In light of the above findings, the following approach might be appropriate to apply to the quantitation of DSE in clinical practice. First, there should be a visual inspection of the images. The eye perceiving motion in all LV segments to be synchronous is highly predictive of normality. When visual inspection suggests there is a regional wall-motion abnormality, velocity data could be used to ascertain if the segmental peak systolic velocity response is abnormal. If abnormal, then ultrasonic deformation indices should then be used to define the ischemic substrate. In hearts with the combination of conduction or rhythm abnormalities and complex wall-motion abnormalities, deformation imaging may be the first line approach to assessing regional function.

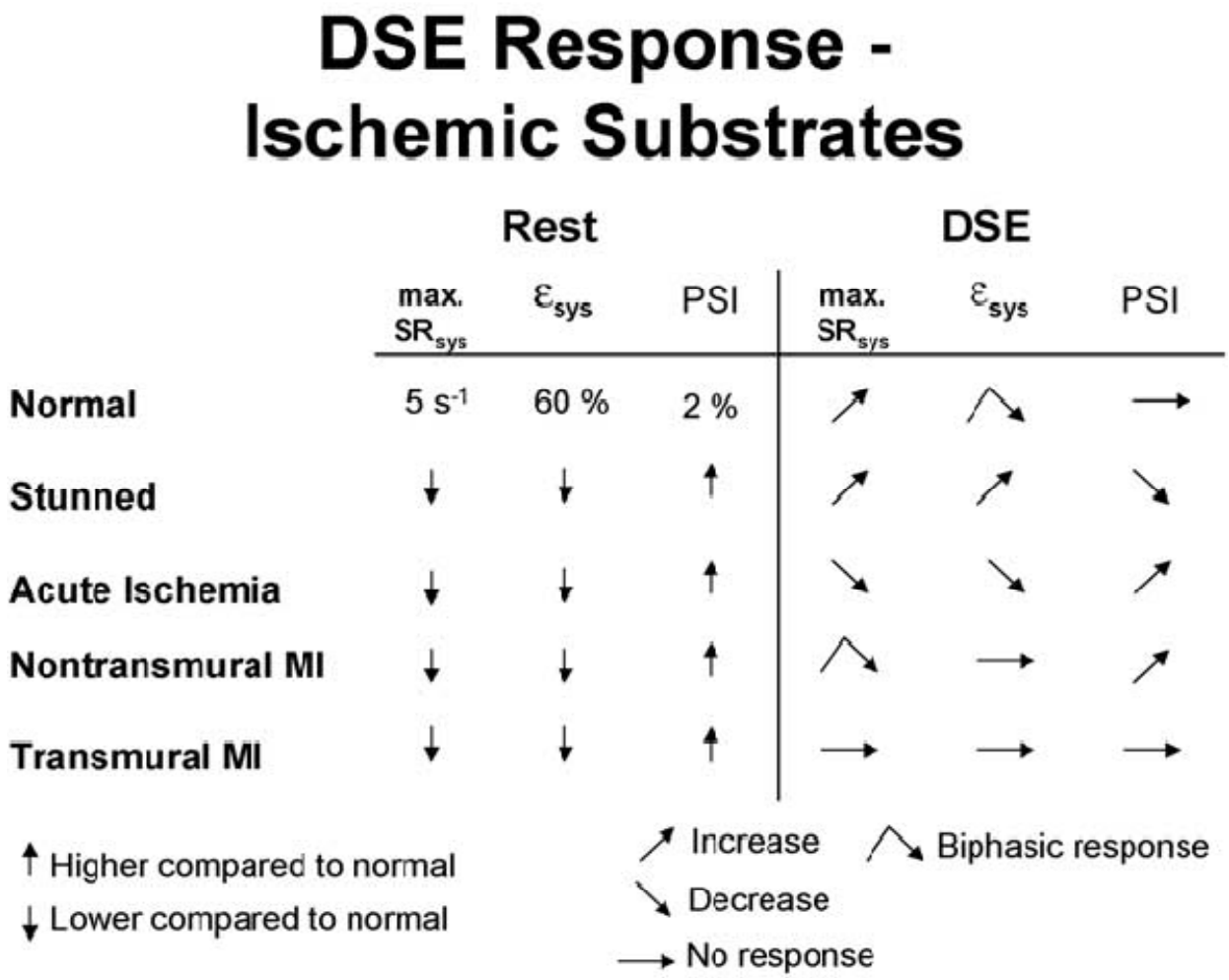


Table 4**:** Strain imaging in various spectrum of Acute Coronary Syndromes assessed by Dobutamine stress

**Valvular Heart Disease**

Valvular heart disease can alter regional Valvular heart disease can alter regional deformation indices in differing ways with changes reflecting the complex interactions of changes in preload/afterload with changes in contractility. A good example of the problems inherent in quantifying and interpreting regional function in valve disease is aortic stenosis. Traditional imaging approaches have been on the basis of the visual interpretation of the combination of endocardial radial motion and radial myocardial thickening. This can be suboptimal as this

disease has its main effect on the subendocardial layer, which is better assessed by measuring long-axis function. Initial clinical experience with ultrasonic deformation indices in patients with aortic stenosis demonstrated that the afterload-related reduction in longitudinal systolic deformation correlated both with aortic valve area and stroke volume. These clinical findings are in keeping with those predicted by the mathematic model of Claus et al.[26] In addition, regional deformation indices could discriminate between patients with and without coronary artery disease who have the same aortic valve area by identifying ischemia-related changes in deformation in the segments at risk. Myocardial velocity profiles could not make this distinction.[36]

**Diastolic Function**

Regional abnormalities in myocardial diastolic motion may be detectable despite mitral and pulmonary vein velocities being normal. Garcia-Fernandez et al[37] already demonstrated in an experimental model of acute ischemia that up to 40% of segments may have measurable regional diastolic motion abnormalities whereas blood pool indices remain normal. It should also be appreciated that changes in regional diastolic function may be expressed differently in the radial versus the longitudinal direction. For example, for basal segments, changes in E' velocities/deformation with increasing filling are more pronounced in the radial direction compared with the longitudinal. One advantage of the new ultrasound deformation SR/strain indices for the study of diastolic events is that they offer very high real-time temporal resolution of deformation (sampling rates of 200 frames/s) compared with other noninvasive imaging modalities. This is important when studying diastole, as very high amplitude, short-lived deformations occur during this time period (this is especially true for untwisting and shape

change during the isovolumic relaxation period). SR imaging has shown the normal sequence of regional changes in deformation during diastole to be complex. Regional lengthening will usually commence in the midinferior septal segment. This early lengthening may start before aortic valve closure. The early midseptal lengthening may have propagated to the apex by the time of mitral valve opening. The basal segments are the last to start to lengthen in early diastole. Their lengthening is associated with the onset of flow into the LV. In contrast, in the free walls, changes in deformation are more variable. After the cessation of early lengthening as a result of early filling, there is a reverse lengthening wave caused by passive recoil, which starts at the apex and spreads toward the base. This recoil is more prominent in young people and has been related to the presence of an audible third heart sound. During diastasis there are usually no measurable changes in deformation. Diastasis is followed by a base-apex wave of lengthening that is caused by atrial filling of the ventricle. This normal pattern may be markedly altered in disease.

**Cardiomyopathies**

A number of studies on the application of velocity, SR, and strain indices to both hypertrophic and dilated cardiomyopathies have been published.[38] In hypertrophic cardiomyopathies, the thick walls make this disease particularly suitable to studies with SR/strain imaging. SR/strain imaging indices have been shown to be better than regional velocity profile data in detecting regional abnormalities in patients with asymmetric septal hypertrophy and in discriminating hypertrophic cardiomyopathy from physiologic hypertrophy. SR/strain imaging has also been shown to be better than either gray-scale M-mode or velocity data in detecting changes in regional function either after septal ablation or in detecting the regression of hypertrophy after

antioxidant treatment for hypertrophic cardiomyopathy. Conversely, applying SR/strain imaging to the study of dilated cardiomyopathies has proved to be very difficult. This is because of a combination of factors: in these hearts the myocardial walls are thin and hyporeflective and the shape of the heart is more spheric. Thus, it is difficult to derive interpretable SR/strain curves because of the combination of poor signal-noise ratio, a small region of interest, and poor alignment of the ultrasound beam to the deformation vector to be interrogated.

**Right Ventricular Function**

Regional right ventricular (RV) velocities, 1-dimensional strain and SR data can also be derived from segments of the RV free wall. To characterize regional RV myocardial function, data can be obtained on radial deformation (by parasternal imaging) and free-wall longitudinal deformation (By apical imaging). Kowalski et al [11] studied regional RV SRs and strain in control subjects and defined segmental velocity/SR/strain profiles and peak values for both radial and longitudinal regional deformation throughout the LV and RV. However, using current methodology, radial SR/starin values proved difficult to measure from the normal thin (6 mm) RV free wall, as the small computational distance, combined with near field imaging artifacts, made accurate postprocessing of radial RV SR/strain values difficult.

**Monitoring Therapy**

The evaluation of new therapeutic strategies that affect ventricular function could benefit from a sensitive, noninvasive measurement technique. Gray-scale echocardiography is the current standard clinical ultrasound approach to assessing LV mass and global LV function. Unfortunately, the sensitivity with which these two parameters can be measured is limited. Thus, the detection of change usually requires long follow-up periods, with change typically

only detectable at group level. The relative insensitivity of gray-scale imaging is a result of the fact that measurement is on the basis of image segmentation by using signal amplitudes. In contrast, SR/strain imaging is potentially more sensitive to change, as it is on the basis of detection of phase shifts and this is inherently less noise sensitive. This advantage was clearly shown in the clinical study of Di Salvo et al [39] in which SR data were able to detect LV mass regression in individual patients with Friedreich's ataxia after 4 months of an antioxidant therapy. This allowed the early detection of both responders and nonresponders. These findings contrasted with both regional velocity (unchanged during treatment) and gray-scale data, both of which could only detect changes in LV mass index at group level after 1 year of therapy. Ultrasoundbased deformation imaging is inherently more sensitive in detecting abnormalities in systolic function and has been confirmed in further clinical studies including amyloid, Fabry's disease, type 2 diabetes, aging, Duchenne's muscular dystrophy and anthracycline therapy.

**The Potential Role of SR/Strain Imaging in Congenital Heart Disease**

Deformation imaging has been used to monitor LV function in patients with abnormal left coronary artery arising from the pulmonary artery both before and after coronary reimplantation, [40,41] and in the late follow-up. Weidemann et al[42] also used SR/strain imaging to assess regional RV function late postrepair of tetralogy of Fallot and showed a homogeneous reduction in deformation properties both within the RV free wall (reflecting the degree of RV dilatation) and throughout all LV walls for both longitudinal and radial function. Conversely, myocardial velocities in the LV posterior wall were significantly increased most probably because of the paradoxical motion of the interventricular septum and abnormal tethering of LV

segments to the dilated RV. SR and strain measurements have also been used to identify and quantify normal and abnormal systemic ventricle regional function in children after an atrial switch procedure.

## AIM OF THE STUDY

To assess longitudinal strain of individual segments and global LV function by strain imaging in patients with acute ST-elevation myocardial infarction and to compare them with wall motion score index and Simpson`s method respectively.

**MATERIALS & METHODS**:

**Study Population**: The study was conducted in patients admitted to the intensive care unit of Govt. Rajaji hospital, Madurai. Fifty two patients with a diagnosis of Acute ST elevation anterior wall MI were studied. Thirty two patients had an acute anterior wall MI and twenty had inferior wall MI. Age group of study in the AWMI group was 52.7± 9.4, in the IWMI group it was 50.7 ± 9.1. 22% of AWMI patients and 20% in the IWMI group were females. 32% patients in the AWMI and 30% in IWMI were diabetic. The prevalence of systemic hypertension in the AWMI was higher 43% and in the IWMI group was 20%. Smoking prevalence was substantial in both MI groups, 75% and 87% in AWMI and IWMI respectively. 75% in the AWMI and 85% in the IWMI group were eligible candidate were thrombolysed.

**Inclusion Criteria**:

1. Patients with Acute ST elevation MI- Anterior wall and Inferior wall

**Exclusion Criteria**:

1. Previous Myocardial Infarction
2. Patients with unstable rhythm (Atrial Fibrillation, Heart blocks, Ventricular Tachycardia)
3. Patients with associated Valvular Heart Disease.
4. Patients on Permanent Pacemakers
5. Patients with Congenital heart diseases.

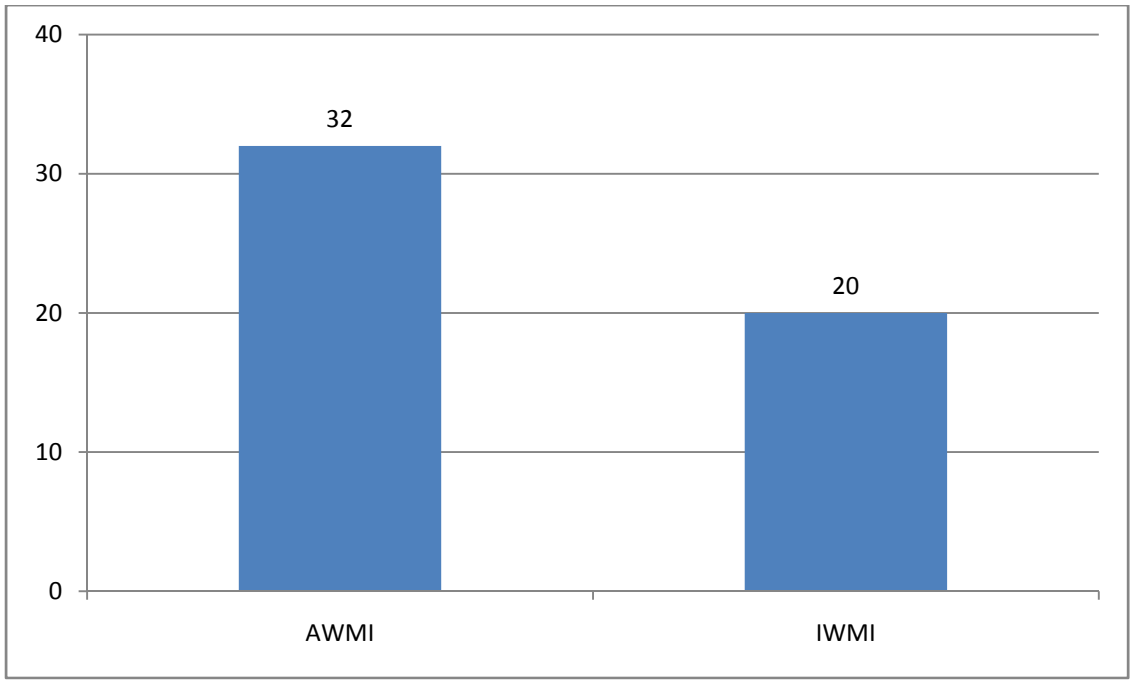


**Localization of MI in the patient population.**

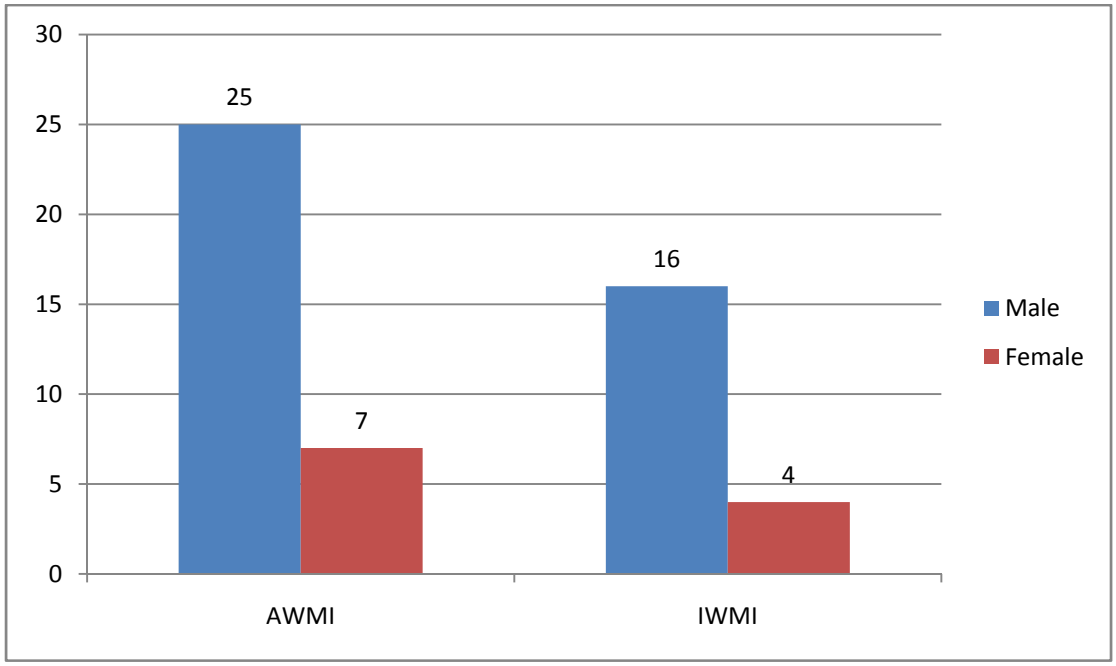


**Gender Distribution of the study population**

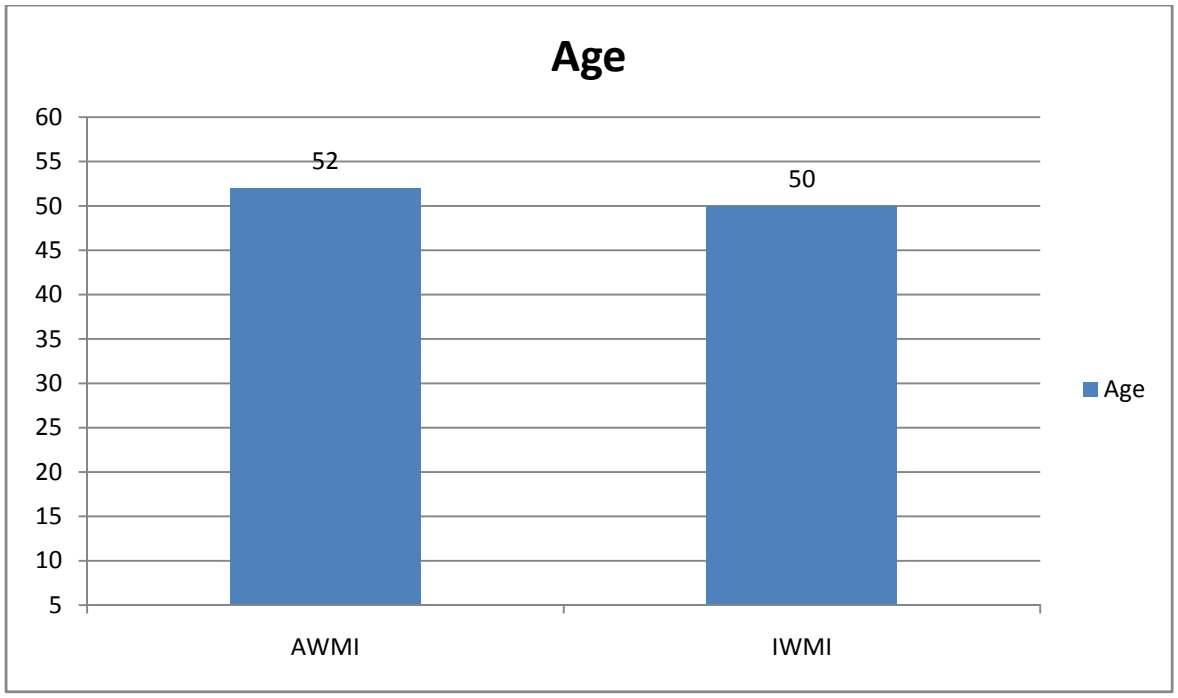


**Age distribution of the population**

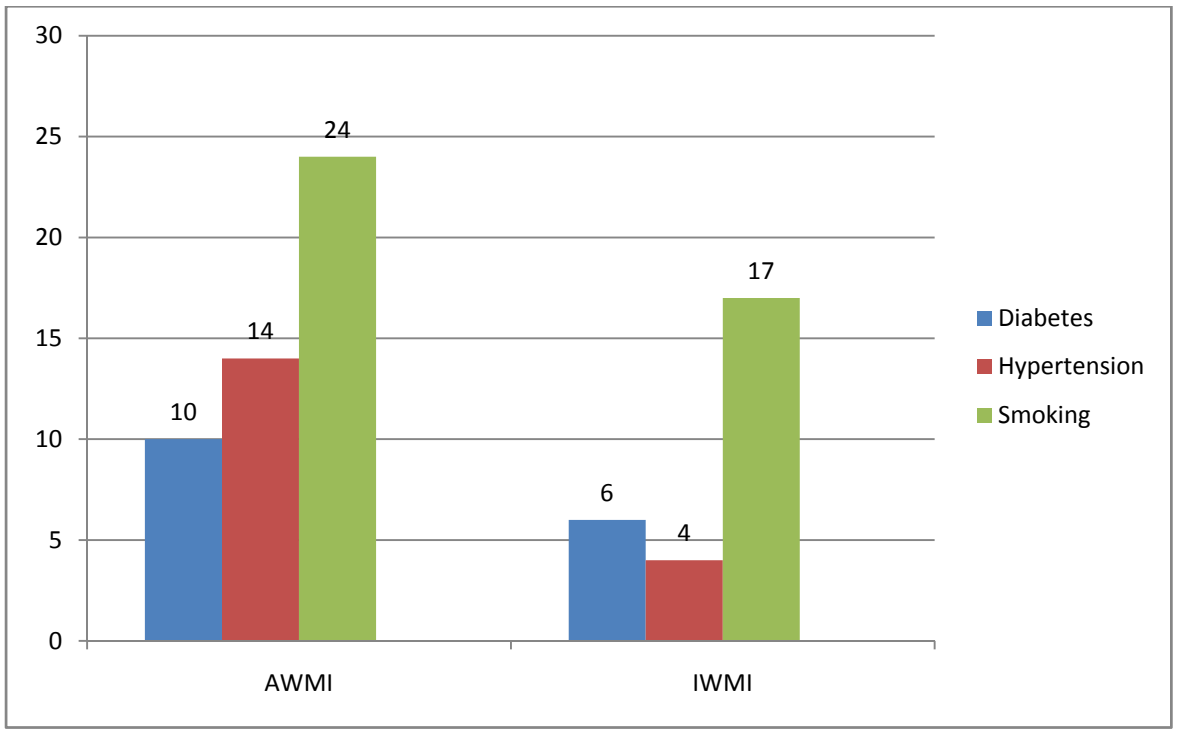


**Prevalence of Risk Factors.**

**Echocardiography**:

A detailed Echocardiographic evaluation for regional wall motion analysis was done on all patients using Philips iE33 machine.

Wall Motion Score Index: Two-dimensional (2-D) images of the LV were obtained from the apical four-chamber view and two chamber view. Wall motion was assessed by analyses of movement and thickening of the myocardium in the three septal and three lateral segments in the apical four-chamber and two chamber views. A score was given to each segment: 1 = normal, 2 = hypokinesia, 3 = akinesia, 4 = dyskinesia, 5= aneurysm. A wall motion score index (WMSI) was calculated as the sum of scores over number of analyzed segments[8] All analyses were performed from three regions along the interventricular septum (apical, mid- and basal septum) and in the corresponding regions on lateral wall.

Simpson method derived ejection fraction was calculated in all patients. A biplane derived EF is obtained in all patients in A2C and A4C views. This was done by tracking the endocardial border of LV in the above mentioned views and obtaining the end systolic and end diastolic volumes. The stroke volume is calculated and the %EF obtained.

**Strain** (e) is originally defined as a dimensionless quantity produced by the application of a stress. It represents the fractional or percentages change from the original or unstressed dimension. This equals the relative change of segmental length occurring between the reference state (end-diastole) and the state of deformation (end-systole) expressed in percentage of end-diastolic length.

The strain imaging in this study was obtained with the patient in the left lateral decubitus position using a commercially available system (PHILIPS iE33). The images were acquired using a 3.5-MHz transducer at a depth of 16 cm in the parasternal and apical views (2- and 4-chamber images). All echocardiographic data were analyzed off-line using Tissue motion Quantification (TMQ advanced) method of the Q-Lab software. Analysis of individual myocardial segments was the principal component of the study. Apical 4 chamber view analyzed the basal, mid, apical septal and lateral segments. Apical 2

chamber view analyzed the basal, mid, apical inferior and anterior segments. Left ventricular apex was analyzed in both views. The peak systolic longitudinal strain was measured. The global LV longitudinal strain was assessed with this commercially available technique, myocardial tissue deformation is calculated using speckle tracking from 2D gray-scale images (2- and 4-chamber views). Aortic valve closure timing was marked in the selected views, and 3 points were anchored inside the myocardial tissue, 2 placed at the basal segments along the mitral valve annulus and 1 at the apex. These points triggered the automatic process, which analyzed myocardial motion by tracking features (natural acoustic tags). The percentage of wall lengthening and shortening was displayed for each plane and represented longitudinal strain. The results of all planes were then combined, which presents the analysis for each segment along with a global strain value for the entire left ventricle.

The mean frame rate of the obtained images was 70 frames/s (range 40 to 100). Only one cardiac cycle needs to be acquired for the off line processing but the major issue here is the high quality image with the maximum possible resolution. The necessity of high image quality is a major limitation for routine clinical applicability in all patients. At present, the optimal frame rate for speckle tracking seems to be 50–70 frames per second (FPS), which is however lower compared to TDI (180 FPS). Using higher frame rates could reduce the under-sampling problem, but this will result in a reduction of spatial resolution and consequently less optimal region of interest (ROI) tracking. Low frame rate increases the spatial resolution, but because speckle tracking software uses a frame-by-frame approach to follow the myocardial movement and searches each consecutive frame for a speckle pattern closely resembling and in close proximity to the reference frame, with too low a frame rate the speckle pattern could be outside the search area, again resulting in poor tracking . It is also important to know that different tracking algorithms potentially produce different results and therefore it should be kept in mind that a periodical update of the software package conceivably influences reference values. The lack of angle

dependency is a great advantage of non- Doppler 2D-strain imaging in comparison to TDI-derived strain data.

In our study the automated tracking by the machine may either be accepted as such or altered according to the wish of the operator if the automated tracking is not satisfactory. This is accomplished by using the reference point's function and adjusting the same to match the segment correctly. The strain was obtained at the peak systole by ECG gating. Placing the cursor at the individual curve at the peak systolic line gives the value of longitudinal strain of individual segment. Thus the values are calculated for all the segments and displayed separately is a table. The global strain derived is automatically displayed by the software and if the tracking is acceptable, this value may be taken as such. In other cases where the tracking is not satisfactory the image settings are adjusted until a proper tracking is obtained. The image taken at the apical long axis view was consistently measured as that of the septum and lateral wall by the software though it did not mean it. Hence for the sake of questionable acceptability in recognized forums, the values in the particular view were ignored. This might be considered as one of the major limitation of the study.

The Longitudinal strain obtained is depicted along the Y-axis of the image as % shortening/lengthening. The value can be manually calculated by noting the excursion of the plot of individual myocardial segment. A good excursion of the plot along the X-Y axis is indicative of good myocardial strain and hence a good LV function of the segment concerned. When there is uniformly good excursion of all segments it indicates normal global LV function.

## RESULTS

**Statistical analysis:** Data analysis was done with the help of computer using Epidemiological Information Package (EPI 2008) developed by Center for Disease Control, Atlanta. Using this software, range, frequencies, percentages, means, standard deviations, coefficient of correlation and 'p' values were calculated. A 'p' value less than 0.05 is taken to denote significant relationship .If the coefficient of correlation is more than or equal to $\pm$ 0.5, then there exists significant relationship between the two variables. A coefficient of correlation of 0.8 or more signifies that a very strong relationship exists between the two variables.

Peak systolic Longitudinal strain was reduced in the individual ischemic myocardial segments and uniformly normal in the non-ischemic segments.[Fig.1] In anterior wall MI patients the WMSI was increased and strain reduced in mid, apical septum; LV apex; basal, mid and apical lateral; basal, mid and apical anterior segments. Statistical analysis of the data revealed positive correlation(>0.50) between the values obtained by WMSI and strain in the basal, mid and apical lateral segments ; basal, mid and apical anterior. Even though the mid septal ,apical septal and apical segments showed reduced strain, statistical positive correlation was lacking in these areas. Similarly the basal septal, mid, apical lateral segments; basal, mid, apical inferior segments showed reduced sterian and increased WMSI. However only the basal septum, basal, mid and apical inferior segments showed positive correlation(>0.5).[Table.1]

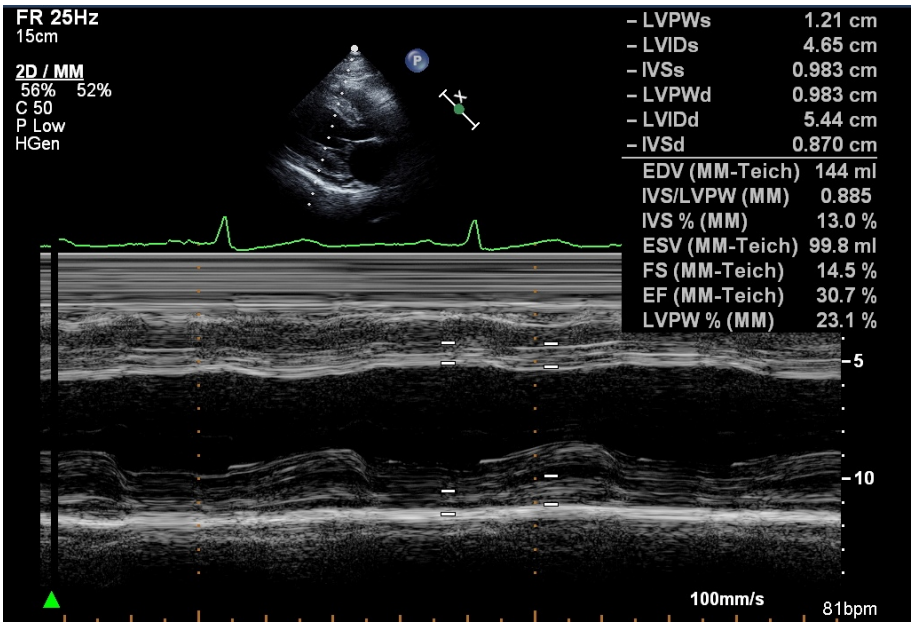


Fig I(a): M-Mode Echo Teichholz method for calculation of EF in a AWMI patient

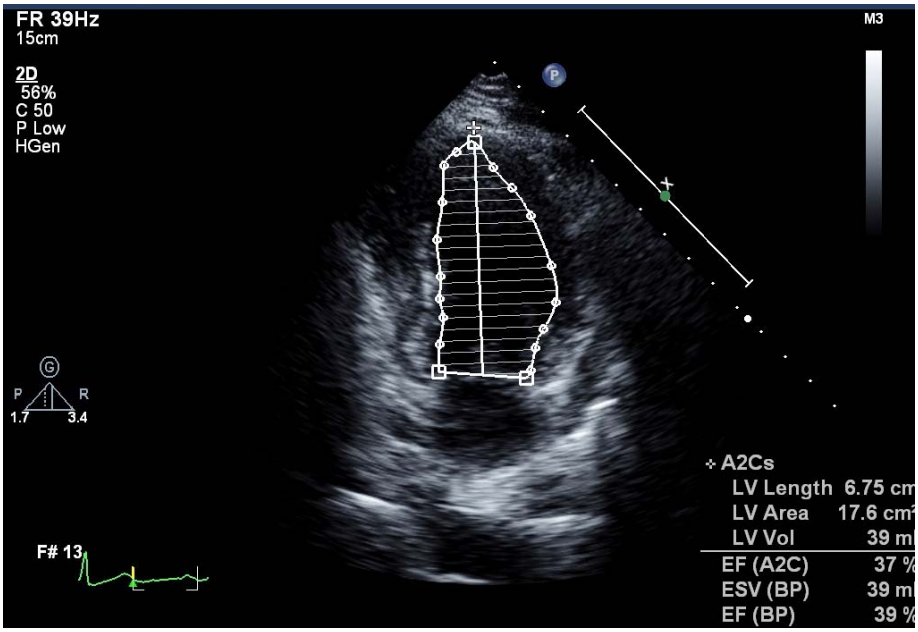


Fig I(b): Simpson`s Bi-plane method for Calculation of EF in the same patient

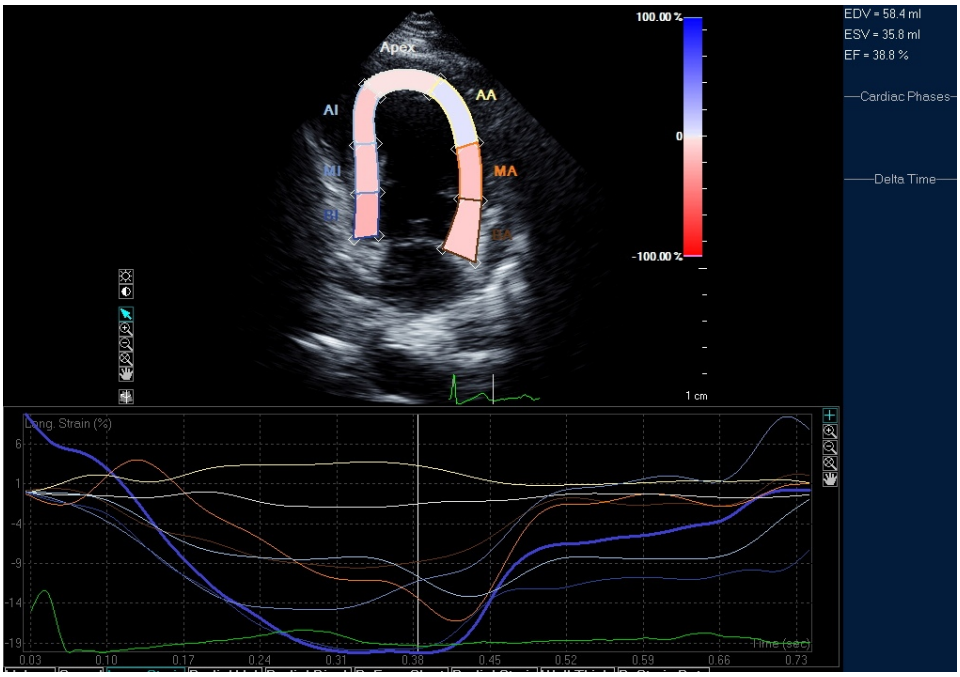


Fig I(c): Longitudinal strain of Anterior and Inferior segments showing reduction of Peak systolic longitudinal strain in the anterior segments and preservation of the same in the inferior segments.

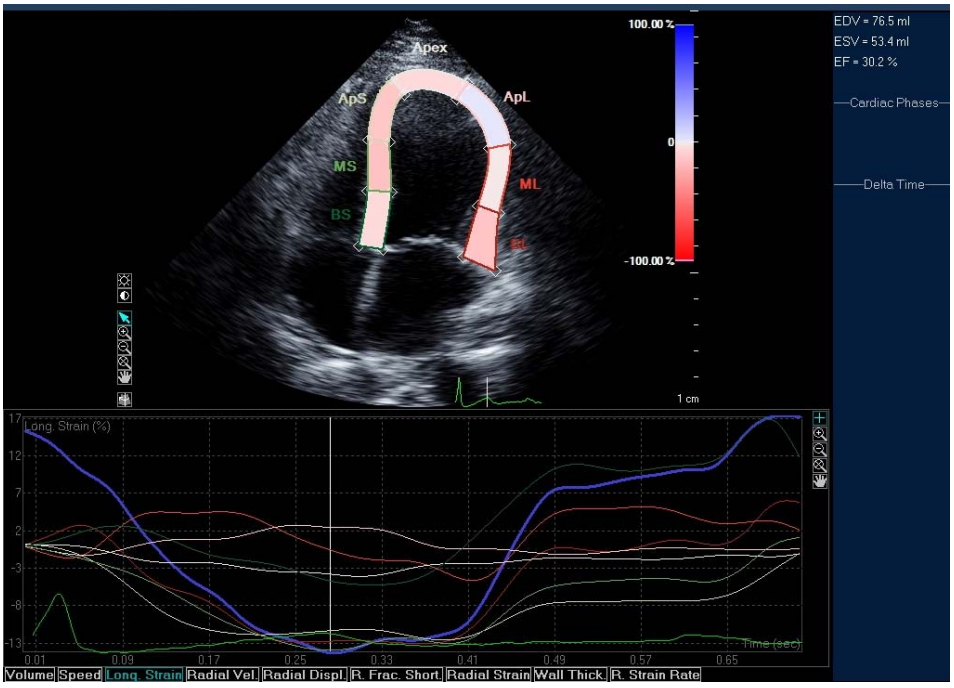


Fig I(d): Longitudinal strain of septal and lateral segments showing reduction of Peak systolic longitudinal strain in the mid-septal, apical and lateral segments and preservation of the same in the basal septum.

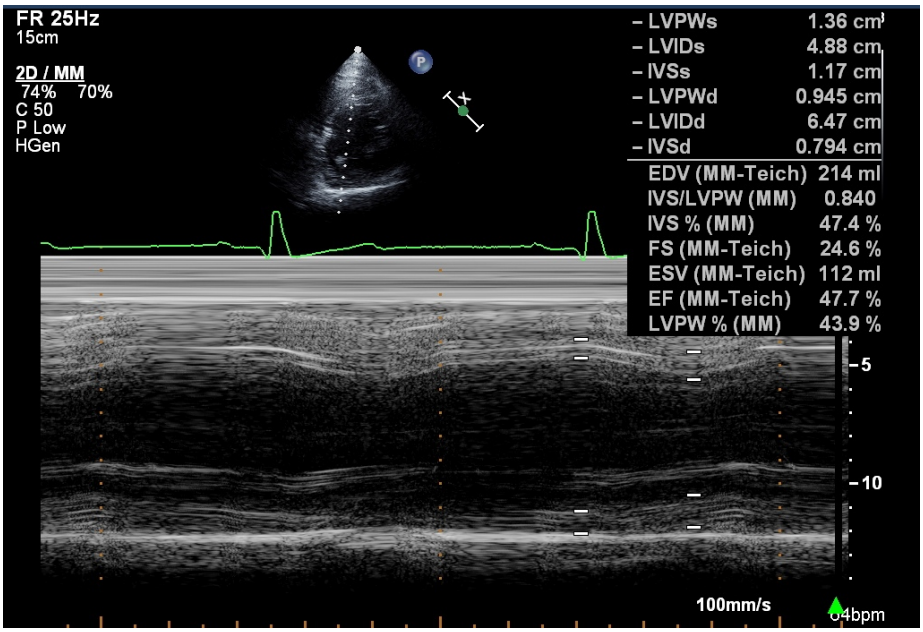


Fig 2(a): LV function obtained by M-Mode Teichholz method in IWMI

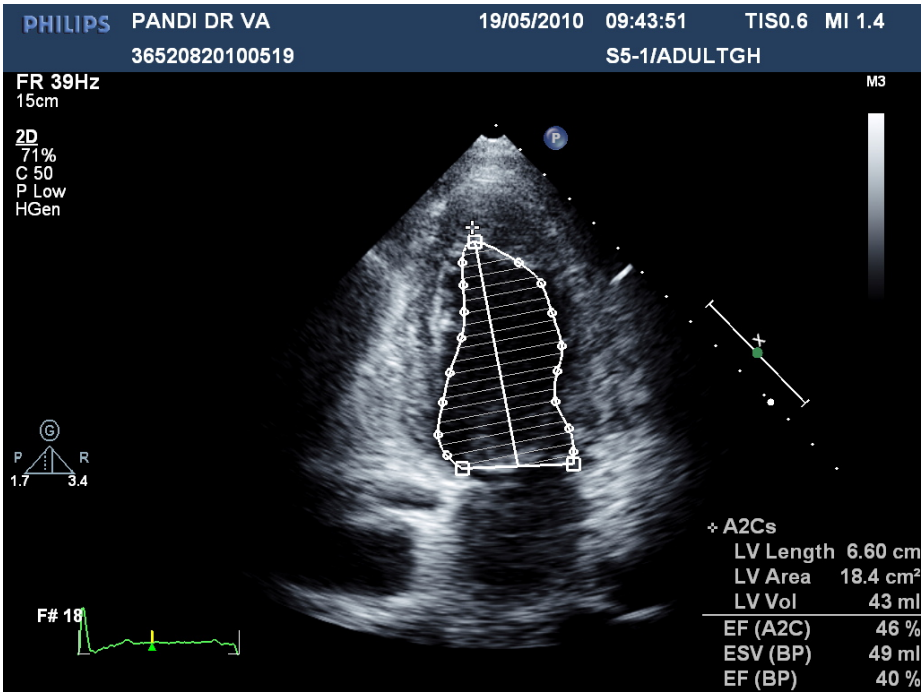


Fig 2(a): Simpson`s method applied in the same patient with IWMI

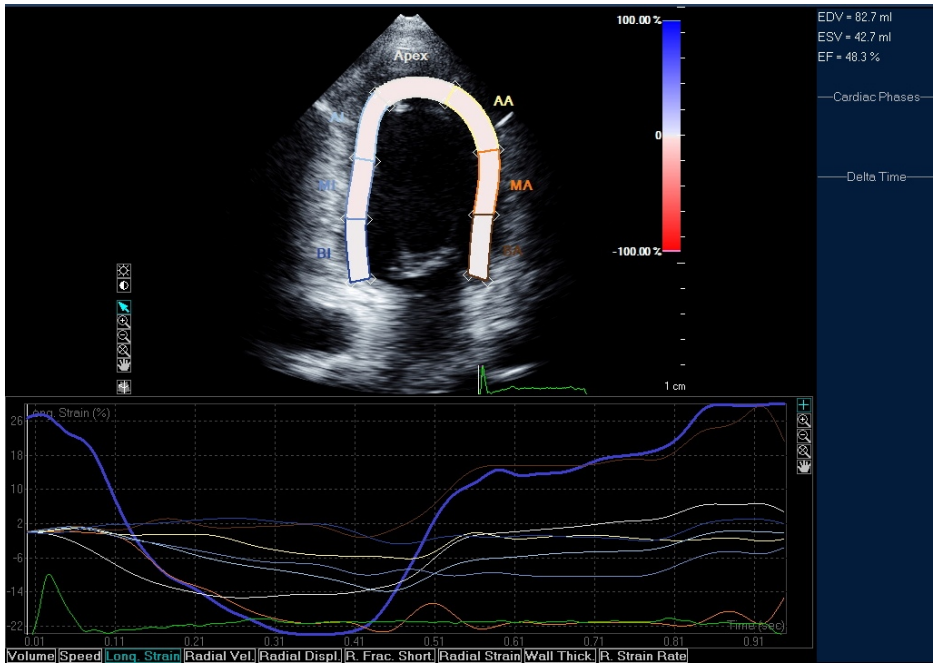


Fig 2(b): Longitudinal Strain in the same patient obtained in Apical 2 chamber view.

| Myocardial Segment | AWMI Group | | | IWMI Group | | |
|---|---|---|---|---|---|---|
| | **WMSI** | **PSLS** | **Correlation Coefficient** | **WMSI** | **PSLS** | **Correlation Coefficient** |
| Basal Septum | 1.28 ± 0.46 | -16.7 ±4.6 | 0.32 | 1.8 ± 0.5 | -10.3 ± 9 | **0.58** |
| Mid Septum | 2.06 ± 0.67 | -7.5 ± 4.5 | 0.42 | 1.35 ± 0.49 | -17.3 ± 4.4 | 0.49 |
| Apical Septum | 2.44 ± 0.5 | -3.0 ± 4.2 | -0.02 | 1.0 ± 0 | -15.1 ± 4.2 | - |
| Basal Lat. | .34 ± 0.55 | -15.9 ± 4.7 | **0.53** | 1.25 ± 0.44 | -17.2 ± 4.1 | 0.44 |
| Mid Lat. | 1.44 ± 0.56 | -11.6 ± 5.5 | **0.68** | 1.45 ± 0.51 | -12.4 ± 4.8 | **0.54** |
| Apical Lat. | 1.81 ± 0.59 | -7.3 ± 5.8 | **0.62** | 1.45 ± 0.51 | -11.6 ± 4.3 | 0.23 |
| Apex | 2.44 ± 0.5 | 0.7 ± 4.9 | 0.28 | 1.0 ± 0 | -15.2 ± 3.3 | - |
| Basal Anterior | 1.5 ± 0.57 | -11.3 ± 6.9 | **0.64** | 1.0 ± 0 | -20 ± 2.6 | - |
| Mid Anterior | 2.38 ± 0.49 | -5 ± 4 | **0.56** | 1.0 ± 0 | -18.2 ± 1.4 | - |
| Apical Anterior | 2.28 ± 0.58 | -3.1 ± 4.5 | **0.52** | 1.0 ± 0 | -17.6 ± 1.93 | - |
| Apical inferior | 1.0 ± 0 | -17 ± 1.8 | - | 2.3 ± 0.47 | -3.25 ± 4.81 | **0.56** |
| Mid inferior | 1.0 ± 0 | -17.8 ± 2.8 | - | 2.35 ± 0.49 | -1.85 ± 5.7 | **0.63** |
| Basal inferior | 1.0 ± 0 | -19 ± 3.1 | - | 2.45 ± 0.51 | -7.15 ± 4.43 | **0.56** |

**Table 1**: Comparison of WMSI and peak systolic longitudinal strain values with coefficient of correlation. The numbers marked in bold show positive correlation (>0.50)

Correlation between 2D Simpson derived EF and strain derived EF was also calculated. There was a positive correlation in the EF between the different modalities.[9] The correlation was strongly positive in the AWMI group with a value of 0.87. The correlation in the IWMI group was also positive at 0.59. [Table. 2]

Individual risk factor analysis revealed that the presence or absence of a particular risk factor did not significantly affect the strain or WMSI as both groups revealed similar trends (p valve >0.05).

| **Group** | **EF (2D) values ascertained by** | | **Correlation coefficient** |
|---|---|---|---|
| | **Simpson method** | **Strain method** | |
| AWMI | 39.1 $\pm$ 8.1 | 38.8 $\pm$ 10.9 | **0.87** |
| IWMI | 44.9 $\pm$ 4.9 | 44.3 $\pm$ 6.0 | **0.59** |

Table 2: Comparison of EF by 2D and Strain methods. Bold numbers indicate positive correlation

## DISCUSSION

Strain imaging measures tissue deformation rather than tissue velocity. It localizes regional wall motion abnormalities as does the conventional methods like wall motion score index and Simpson method. Conventional methods are based on the principle of measuring tissue velocity. Tissue tethering is an inherent disadvantage of these methodologies and cannot be avoided because of the geometric orientation of the myocardial fibers. Hence strain imaging using peak systolic longitudinal strain in acute MI patients may be used to overcome this disadvantage and quantify both wall motion score and overall LV systolic function.

Strain can be measured in all three dimensions as the tissue deforms three dimensionally. Thus the deformation in the longitudinal, radial and circumferential planes can be assessed in a patient with MI. However the Longitudinal fibers are the main fibers distributed in the Sub-endocardial region, the region most susceptible for ischemia. Thus measurement of longitudinal strain is more reasonable in a patient with acute myocardial ischemia.

The Peak systolic Strain is measured in this study because it is the magnitude parameter that corresponds with regional ejection fraction. We depend on the EF derived by the Q-Lab software based on the tissue deformation of individual myocardial segments. Hence the assessment of Peak systolic strain is ideal rather than end-systolic strain which is both timing and magnitude parameter that lacks information about the rate of contraction of individual myocardial fibers.

The results of the study shows that the longitudinal strain in the myocardial segments shows good correlation with the previously well evaluated methods like WMSI and Simpsons

method. Even though the correlation was not uniform as some of the segments namely the mid septum, apical septum and apex showed no statistical correlation, the overall values were reduced in these segments. Similarly in the IWMI group only the basal septal, basal mid and apical inferior segments showed positive correlation. The Basal septum is supplied by the Right Coronary artery and is not involved in AWMI. The strain pattern is not affected in this segment in patients with AWMI. Patients with IWMI show a reduced strain in this segment that correlates with the WMSI of such patients.

In the study by Thor Edwardsen et al[43] Seventeen patients undergoing angioplasty of the left anterior descending coronary artery (LAD) were studied. Left ventricular longitudinal wall motion was assessed by Tissue Doppler Echocardiography and Strain Doppler Echocardiography from the apical four-chamber view before, during and after angioplasty from multiple myocardial segments simultaneously. Segments not supplied by LAD remained unchanged. Tissue Doppler echocardiography showed reduced velocities in all septal segments ($p = 0.05$) during Angioplasty Wall motion score index increased during ischemia ($p=0.05$). It was concluded that the new SDE approach might be a more accurate marker than TDE for detecting systolic regional myocardial dysfunction induced by LAD occlusion. The results of our study correlates well with that of this study mentioned. The ischemia was induced voluntarily in the study by Thor Edwardsen et al whereas we have studied the patients who presented with acute STEMI. This was one of the pioneering studies by the authors early in 2001 regarding the utility of the new modality at that point of time.

In the study by Lene Rosendhal et al[44] in 2010, it was shown that Longitudinal Peak Strain Detects a Smaller Risk Area Than Visual Assessment of Wall Motion in Acute Myocardial

Infarction; In this study, tissue Doppler analysis (peak strain, displacement, mitral annular movement (MAM)) was compared with visual assessment for the study of the correlation of measurements of global, regional and segmental function with final infarct size and transmurality. It was concluded that, in patients with acute STEMI, WMSI, EF, strain, and displacement showed significant changes between the pre- and post PCI exam. In a ROC-analysis, strain had 64% sensitivity at 80% specificity and WMSI around 90% sensitivity at 80% specificity for the detection of scar with transmurality.

Gjesdal et.al[45] showed a higher correlation (0.84) between global strain and scar compared to WMSI and scar (0.70) in patients with chronic myocardial infarction. In their study, 2D-speckle tracking echocardiography was used on patients (mean age 55 yrs) 9 months after MI.

Vartdal et. al[46] found a correlation of 0.77 between strain and infarct size in patients with acute STEMI. The corresponding figure for WMSI and infarct size was r = 0.45. However, these patients were examined 1.5 h after revascularization when ischemic wall motion abnormalities could have declined, possibly faster than changes in strain. Interestingly, they also found that global strain might be a valuable predictor for the total amount of scar and hence might be a clinical tool for risk stratification.

Recently, Gjesdal et.al[47] showed a significant correlation between Mitral Annular Movement, measured in 4 positions, and infarct size ($r = 0.58$, $p < 0.01$) in patients with chronic scar 9 months post AMI.

Sjoli et.al[48] showed a correlation of 0.62 between global strain and infarct size measured within 3.5 h after revascularization. Global strain showed a higher correlation with the size of

myocardial scar compared with LVEF. This result is in line with our study that the global LV function assessment was better correlating rather than the regional assessment.

Ugander et.al[49] confirmed a large variation in LVEF in relation to infarct size and concluded that infarct size cannot be used to predict LVEF. The number of dysfunctional adjacent segments seemed to be a more important determinant on regional wall function than infarct transmurality. This could be caused by extensive hibernation or a compensatory increase in wall motion in healthy parts of scarred ventricles.

Prognostic importance of strain and strain rate after acute myocardial infarction was studied by M. Lousia Antoni et al[50] in their study of 659 patients after AMI. Patients were evaluated using strain, WMSI and LVEF. Strain was independently related to all endpoints and was found to be superior to LV ejection fraction (LVEF) and wall motion score index (WMSI). Patients with global strain and strain rate higher than −15.1% and $-1.06\ s^{-1}$ demonstrated HRs of 4.5 (95% CI 2.1–9.7) and 4.4 (95% CI 2.0–9.5) for all-cause mortality, respectively. Conclusion was that Strain and strain rate provide strong prognostic information in patients after AMI. These novel parameters were superior to LVEF and WMSI in the risk stratification for long-term outcome. This study reiterates the importance of strain imaging in patients with acute myocardial infarction.

Guy Armstrong et al[51] studied the use of Use of Peak Systolic Strain as an Index of Regional Left Ventricular Function. It was concluded that myocardial tissue Doppler velocity is an objective measure of regional left ventricular responses to inotropic stimulation and ischemia, but it is affected by tethering from adjacent segments and translational movement.

Zoran B. Popovic et al[52] in their study `Speckle-tracking echocardiography correctly identifies segmental left ventricular dysfunction induced by scarring' demonstrated that both sensitivity of circumfrential strain($S_{circ}$) and Sensitivity of radial strain($S_{rad}$) significantly decreased after myocardial infarction (*P* _ 0.0001 for both). Study was conducted on rat model. As anticipated, $S_{circ}$ and $S_{rad}$ were lowest in the infracted segments. Multiple linear regression showed that segmental $S_{circ}$ were similarly dependent on segmental fibrosis and end-systolic diameter (*P* _ 0.0001 for both), whereas segmental $S_{rad}$ measurements were more dependent on end-systolic diameter (*P* _ 0.0001) than on percent fibrosis (*P* _ 0.002). Speckle Tracking Echocadiography correctly identifies segmental LV dysfunction induced by scarring that follows myocardial infarction.

## LIMITATIONS

Limitations in this study are that

(1) The 17 segment model as proposed by the American college of cardiology could not be displayed in a bulls eye plot due to the lack of such software in the machine.

(2) Angiographic correlation of region involved was not done.

(3) Correlation was positive (>0.50) in many of the variables compared. However a very strong positive correlation (>0.80) was not obtained in many of the segments.

(4) The study is a single point study and follow up of regional and overall LV function was not compared.

## CONCLUSION

Echocardiography, done using two methods- subjective assessment of wall motion as well as objective measurement of deformation (strain), in patients with acute myocardial infarction detected myocardial regions involved as well as the overall Left Ventricular function. These measurements, the WMSI and Strain correlated with each other with regards to the regional as well as global LV function. Analysis based on coefficient of correlation showed peak systolic longitudinal strain as good as WMSI in this prediction. Thus, advanced technological analysis of wall motion using strain imaging did contribute additional value compared with a conventional assessment such as wall motion score index and Simpson`s method.

# Bibliography

1. Hurst `The Heart', 13th edition, 2011, chapter 60, P 1354.

2. Measurement of Strain and Strain Rate by Echocardiography , Thomas H. Marwick, J Am Coll Cardiol 2006;47:1313–27

3. Schiller NB, Shah PM, Crawford M, et al., American Society of Echocardiography Committee on Standards Subcommittee on Quantitation of Two-Dimensional Echocardiograms. Recommendations for quantitation of the left ventricle by two-dimensional echocardiography. Journal of the American Society of Echocardiography, 1989;2;358â€“367

4. Lieberman AN, Weiss JL, Jugdutt BI, et al. Two-dimensional echocardiography and infarct size: Relationship of regional wall motion and thickening to the extent of myocardial infarction in the dog. Circulation, 1981;63:739-746.

5. Oh JK, Gibbons RJ, Christian TF, et al. Correlation of regional wall motion abnormalities detected by two-dimensional echocardiography with perfusion defect determined by technetium 99m sestamibi imaging in patients treated with reperfusion therapy during acute myocardial infarction. American Heart Journal, 1996;131:32-37.

6 Oh JK, The Echo manual, 3rd edition, Coronary Artery Disease and Acute Myocardial Infarction, P.155.

7. Schiller NB. Ejection fraction by echocardiography: The full monty or just a peep show? American Heart Journal, 2003;146:380â€“382

8. Grayburn PA, Appleton CP, DeMaria AN, et al, BEST Trial Echocardiographic Substudy Investigators. Echocardiographic predictors of morbidity and mortality in patients with advanced heart failure: The Beta-blocker Evaluation of Survival Trial (BEST). Journal of the American College of Cardiology, 2005;45:1064â€“1071.

9. Quinones MA, Waggoner AD, Reduto LA, et al. A new, simplified and accurate method for determining ejection fraction with two-dimensional echocardiography. Circulation, 1981;64:744â€“753.

10. Feigenbaum`s Echocardiography, 6th ed. Coronary Artery disease, P.443.

11. Kowalski M, Kukulski T, Jamal F, et al. Can natural strain and strain rate quantify regional myocardial deformation? A study in healthy subjects. Ultrasound Med Biol 2001;27:1087–97.

12. Heimdal A, Stoylen A, Torp H, Skjaerpe T. Real-time strain rate imaging of the left ventricle by ultrasound. J Am Soc Echocardiogr 1998;11:1013–9.

13. Reisner SA, Lysyansky P, Agmon Y, Mutlak D, Lessick J, Friedman Z. Global longitudinal strain: a novel index of left ventricular systolic function. J Am Soc Echocardiogr 2004;17:630 –3.

14. Sutherland GR, Di Salvo G, Claus P, D'hooge J, Bijnens B. Strain and strain rate imaging: a new clinical approach to quantifying regional myocardial function. J Am Soc Echocardiogr 2004;17:788–802.

15. Armstrong G, Pasquet A, Fukamachi K, Cardon L, Olstad B, Marwick T. Use of peak systolic strain as an index of regional left ventricular function: comparison with tissue Doppler velocity during dobutamine stress and myocardial ischemia. J Am Soc Echocardiogr 2000;13:731–7.

16. Abraham TP, Nishimura RA, Holmes DR Jr., Belohlavek M, Seward JB. Strain rate imaging for assessment of regional myocardial function: results from a clinical model of septal ablation. Circulation 2002;105: 1403–6.

17. Storaa C, Aberg P, Lind B, Brodin LA. Effect of angular error on tissue Doppler velocities and strain. Echocardiography 2003;20:581–7.

18. Urheim S, Edvardsen T, Torp H, Angelsen B, Smiseth OA. Myocardial strain by Doppler echocardiography. Validation of a new method to quantify regional myocardial function. Circulation 2000; 102:1158–64.

19. Edvardsen T, Gerber BL, Garot J, Bluemke DA, Lima JA, Smiseth OA. Quantitative assessment of intrinsic regional myocardial deformation by Doppler strain rate echocardiography in humans: validation against three-dimensional tagged magnetic resonance imaging. Circulation 2002;106:50–6.

20. Leitman M, Lysyansky P, Sidenko S, et al. Two-dimensional strain—a novel software for real-time quantitative echocardiographic assessment of myocardial function. J Am Soc Echocardiogr 2004;17: 1021–9.

21. Kaluzynski K, Chen X, Emelianov SY, Skovoroda AR, O'Donnell M. Strain rate imaging using two-dimensional speckle tracking. IEEE Trans Ultrason Ferroelectr Freq Control 2001;48:1111–

22. Notomi Y, Lysyansky P, Setser RM, et al. Measurement of ventricular torsion by two-dimensional ultrasound speckle tracking imaging. J Am Coll Cardiol 2005;45:2034–41.

23. Abraham TP, Belohlavek M, Thomson HL, et al. Time to onset of regional relaxation: feasibility, variability and utility of a novel index of regional myocardial function by strain rate imaging. J Am Coll Cardiol 2002;39:1531–7.

24. Sun JP, Popovic ZB, Greenberg NL, et al. Noninvasive quantification of regional myocardial function using Doppler-derived velocity, displacement, strain rate, and strain in healthy volunteers: effects of aging. J Am Soc Echocardiogr 2004;17:132– 8.

25. Brawnwald`s Heart Disease 8th Ed, Chapter on Echocardiography

26. Claus P, Bijnens B, Weidemann F, Dommke C, Bito V, Heinzel F, et al. Post systolic thickening in ischaemic myocardium: a simple mathematical model for simulating regional deformation. Functional imaging and modelling of the heart. Lect Notes Comput Sci 2001;2230:134-9.

27. Weidemann F, Jamal F, Sutherland GR, Claus P, Kowalski M, Hatle L, et al. Myocardial function defined by strain rate and strain during alterations in inotropic states and heart rate.AmJ Physiol Heart Circ Physiol 2002;283:H792-9.

28. Kvitting JPE, Wigstrøm L, Strotmann JM, Sutherland GR. How accurate is visual assessment of synchronicity in myocardial motion? An in vitro study with computer simulated regional delay in myocardial motion. Clinical implications for rest and stress echocardiography studies. J Am Soc Echocardiogr 1999;12:698-705.

29. Voigt JU, Arnold MF, Karlsson M, Hubbert L, Kulkulski T, Hatle L, et al. Assessment of regional longitudinal myocardial strain rate derived from Doppler myocardial imaging indexes in normal and infracted myocardium. J Am Soc Echocardiogr 2000;13:588-98.

30. Firstenberg MS, Greenberg NL, Smedira NG, Castro P, Thomas JD, Garcia MJ. The effects of acute coronary occlusion on noninvasive echocardiographic derived systolic and diastolic myocardial strain rates. Curr Surg 2000; 57:466-72.

31. Armstrong G, Pasquet A, Fukamachi K, Cardon L, Olstad B, Marwick T. Use of peak systolic strain as an index of regional left ventricular function: comparison with tissue Doppler velocity during dobutamine stress and myocardial ischemia. J Am Soc Echocardiogr 2000;13:731-7.

32. Jamal F, Strotmann J, Weidemann F, Kukulski T, D'hooge J, Bijnens B, et al. Non-invasive quantification of contractile reserve of stunned myocardium by ultrasonic strain rate and strain. Circulation 2001;104:1059-65.

33. Kukulski T, Jamal F, D'Hooge J, Bijnens B, De Scheerder I, Sutherland GR. Acute changes in systolic and diastolic events during clinical coronary angioplasty: a comparison of regional velocity, strain rate, and strain measurement. J Am Soc Echocardiogr 2002;15:1-12.

34. Hoffmann R, Altiok E, Nowak B, Heussen N, Kuhl H, Kaiser HJ, et al. Strain rate measurement by Doppler echocardiography allows improved assessment of myocardial viability in patients with depressed left ventricular function. J Am Coll Cardiol 2002;39:443-9.

35. Voigt J-U, Exner B, Schmiedehausen K, Huchzermeyer C, Reulbach U, Nixdorff U, et al. Strain rate imaging during dobutamine stress echocardiography provides objective evidence of inducible ischemia. Circulation 2003;107:2120-6.

36. Kowalski M, Herbots L, Weidemann F, Breithardt O, Strotmann J, Davidavicius G, et al. One-dimensional ultrasonic strain and strain rate imaging: a new approach to the quantitation of regional myocardial function in patients with aortic stenosis. Ultrasound Med Biol 2003;29:1085-92.

37. Garcia-Fernandez MA, Azevedo J, Moreno M, Bermejo J, Moreno R. Regional left ventricular diastolic dysfunction evaluated by pulsed-tissue Doppler echocardiography. Echocardiography 1999;16:491-500.

38. Weidemann F, Mertens L, Gewillig M, Sutherland GR. Quantitation of localized abnormal deformation in asymmetric non-obstructive hypertrophic cardiomyopathy: a velocity, strain rate, and strain Doppler myocardial imaging study. Pediatr Cardiol 2001;22:534-7.

39. Di Salvo G, Weideman F, Mertens L, Eyskens B, Davidavicius G, Bijnens B, et al. The results of long-term Idebenone therapy for myocardial involvement in Friedreich's ataxia: a strain and strain rate imaging study [abstract]. Eur Heart J 2002;4:231.

40. Mertens L, Weidemann F, Sutherland GR. Left ventricular function in abnormal left coronary artery arising from the pulmonary artery pre and post repair: the potential benefits of ultrasound-based regional strain and strain rate imaging. Cardiol Young 2001;11:79-83.

41. Di Salvo G, Eyskens B, Claus P, D'hooge J, Bijnens B, Suys B, et al. Late post repair ventricular function in patients with origin of the left main coronary artery from the pulmonary trunk. Am J Cardiol 2004;93:506-8.

42. Weidemann F, Eyskens B, Mertens L, Dommke C, Kowalski M, Simmons L, et al. Quantification of regional right and left ventricular function by ultrasonic strain rate and strain indexes after surgical repair of tetralogy of Fallot. Am J Cardiol 2002; 90:133-8.

43. Thor Edvardsen, MD, Helge Skulstad, MD, Regional Myocardial Systolic Function During Acute Myocardial Ischemia Assessed by Strain Doppler Echocardiography, J Am Coll Cardiol 2001;37:726–30

44. Lene Rosendahl, MD; Peter Blomstrand, MD; Lars Brudin, MD, PhD; Tim Tödt, MD; Jan E. Engvall, MD, PhD; Longitudinal Peak Strain Detects a Smaller Risk Area Than Visual Assessment of Wall Motion in Acute Myocardial Infarction From Cardiovascular Ultrasound 2010

45. Gjesdal O, Hopp E, Vartdal T, Lunde K, Helle-Valle T, Aakhus S, Smith HJ, Ihlen H, Edvardsen T: Global longitudinal strain measured by two-dimensional speckle tracking echocardiography is closely related to myocardial infarct size in chronic ischaemic heart disease. *Clin Sci (Lond)* 2007, 113(6):287-296.

46. Vartdal T, Brunvand H, Pettersen E, Smith HJ, Lyseggen E, Helle-Valle T, Skulstad H, Ihlen H, Edvardsen T: Early prediction of infarct size by strain Doppler echocardiography after coronary reperfusion. *J Am Coll Cardiol* 2007, 49(16):1715-1721.

47. Gjesdal O, Vartdal T, Hopp E, Lunde K, Brunvand H, Smith HJ, Edvardsen T: Left ventricle longitudinal deformation assessment by mitral annulus displacement or global longitudinal strain in chronic ischemic heart disease: are they interchangeable?. *J Am Soc Echocardiogr* 2009, 22(7):823-830

48. Sjoli B, Orn S, Grenne B, Vartdal T, Smiseth OA, Edvardsen T, Brunvand H: Comparison of left ventricular ejection fraction and left ventricular global strain as determinants of infarct size in patients with acute myocardial infarction. *J Am Soc Echocardiogr* 2009, 22(11):1232-1238.

49. Ugander M, Ekmehag B, Arheden H: The relationship between left ventricular ejection fraction and infarct size assessed by MRI. *Scand Cardiovasc J* 2008, 42(2):137-145

50. M. Louisa Antoni, Prognostic importance of strain and strain rate after acute myocardial infarction Eur Heart J (2010) 31 (13): 1640-1647

51. Guy Armstrong Agnes Pasquet, Use of Peak Systolic Strain as an Index of Regional Left Ventricular Function: Comparison with Tissue Doppler Velocity During Dobutamine Stress and Myocardial Ischemia; Am Soc Echocardiogr 2000;13:731-7

52. Oliver Turschner, The sequential changes in myocardial thickness and thickening which occur during acute transmural infarction, infarct reperfusion and the resultant expression of reperfusion injury European Heart Journal (2004) 25, 794–803

## TABLE FOR ANTERIOR WALL MI

| | | | | | | | | | | WALL MOTION SCORE INDEX | | | | | | | | | | | | | | PEAK SYSTOLIC LONGITUDINAL STRAIN | | | | | | | | | | | | |
|---|---|---|---|---|---|---|---|---|---|---|---|---|---|---|---|---|---|---|---|---|---|---|---|---|---|---|---|---|---|---|---|---|---|---|---|---|
| S.No | Name | Age/Sex | DM | SHT | Smokir | Other | MI | SK | Resul | BS | MS | ApS | Apex | ApL | ML | BL | BA | MA | ApA | BI | MI | ApI | imps | BS | MS | ApS | Apex | ApL | ML | BL | BA | MA | ApA | BI | MI | ApI | oy Strain |
| 1 | Ammasi | 64/M | Y | Y | Y | - | AW | Y | F | 2 | 2 | 3 | 3 | 1 | 1 | 1 | 2 | 3 | 1 | 1 | 1 | 1 | **38** | -9 | -4 | -4 | -2 | -16 | -17 | -20 | -9 | -8 | -4 | -14 | -15 | -18 | **43** |
| 2 | Pannerselvam | 52/M | N | N | Y | F/H | AW | Y | S | 1 | 1 | 2 | 2 | 1 | 1 | 1 | 1 | 2 | 2 | 1 | 1 | 1 | **38** | -16 | -10 | -8 | -8 | -17 | -17 | -19 | -17 | -4 | -5 | -18 | -16 | -20 | **33** |
| 3 | Dellikumar | 39/M | N | N | Y | HC | AW | Y | S | 2 | 3 | 3 | 3 | 2 | 1 | 1 | 1 | 2 | 2 | 1 | 1 | 1 | **40** | -24 | -10 | -10 | -2 | -14 | -19 | -25 | -15 | -4 | -8 | -22 | -20 | -18 | **51** |
| 4 | Mustafa K Batcha | 60/M | Y | Y | N | - | AW | N | - | 1 | 3 | 3 | 3 | 2 | 1 | 1 | 2 | 3 | 3 | 1 | 1 | 1 | **32** | -11 | -2 | 3 | 6 | -5 | -16 | -14 | -2 | 0 | 5 | -26 | -21 | -20 | **23** |
| 5 | Manselan | 54/M | N | N | Y | HC | AW | N | - | 1 | 2 | 2 | 2 | 1 | 1 | 1 | 1 | 2 | 2 | 1 | 1 | 1 | **50** | -25 | -14 | -6 | -6 | -17 | -22 | -21 | -26 | -10 | -4 | -24 | -20 | -19 | **45** |
| 6 | Angaiyyan | 55/M | N | Y | Y | - | AW | Y | S | 1 | 1 | 2 | 2 | 1 | 1 | 1 | 1 | 2 | 2 | 1 | 1 | 1 | **54** | -22 | -18 | -8 | -11 | -18 | -16 | -21 | -26 | -4 | -10 | -20 | -19 | -17 | **48** |
| 7 | Sivalingam | 58/M | N | Y | Y | | AW | Y | | 1 | 2 | 2 | 2 | 2 | 2 | 2 | 1 | 2 | 2 | 1 | 1 | 1 | **55** | -22 | -12 | 4 | 4 | -4 | -4 | -6 | -22 | -10 | -10 | -24 | -18 | -14 | **58** |
| 8 | Chinnaadakki | 41/F | N | N | N | - | AW | Y | S | 1 | 2 | 3 | 3 | 2 | 1 | 1 | 2 | 3 | 3 | 1 | 1 | 1 | **42** | -20 | -6 | -2 | 2 | -8 | -18 | -21 | -12 | -4 | -6 | -20 | -24 | -16 | **55** |
| 9 | Subbiah | 48/M | N | N | Y | - | AW | Y | F | 2 | 3 | 3 | 3 | 3 | 2 | 1 | 3 | 3 | 3 | 1 | 1 | 1 | **26** | -11 | -4 | -4 | 1 | -5 | -8 | -12 | -2 | 0 | 4 | -14 | -14 | -16 | **21** |
| 10 | Thanipiravi | 60/M | Y | Y | N | HC | AW | N | - | 1 | 1 | 2 | 2 | 1 | 1 | 1 | 1 | 2 | 2 | 1 | 1 | 1 | **48** | -18 | -6 | -10 | -12 | -16 | -16 | -17 | -13 | -4 | 0 | -17 | -16 | -15 | **44** |
| 11 | Vedappan | 40/M | N | Y | N | - | AW | N | - | 1 | 1 | 2 | 2 | 2 | 1 | 1 | 1 | 2 | 2 | 1 | 1 | 1 | **46** | -19 | -10 | -5 | 2 | -2 | -15 | -16 | -14 | -9 | -6 | -16 | -14 | -16 | **51** |
| 12 | Nagarathinam | 45/F | Y | Y | N | - | AW | N | - | 2 | 2 | 2 | 2 | 2 | 2 | 2 | 2 | 2 | 2 | 1 | 1 | 1 | **38** | -10 | -6 | -2 | 2 | -4 | -4 | -10 | -4 | -5 | -1 | -18 | -17 | -16 | **33** |
| 13 | Gandhimathi | 42/F | Y | N | N | - | AW | Y | S | 1 | 2 | 2 | 2 | 2 | 2 | 1 | 1 | 2 | 2 | 1 | 1 | 1 | **40** | -16 | -4 | 2 | 4 | -6 | -5 | -14 | -10 | -8 | -4 | -19 | -19 | -15 | **34** |
| 14 | Rahamtulla | 56/M | N | N | Y | - | AW | Y | F | 1 | 2 | 3 | 3 | 2 | 2 | 1 | 2 | 3 | 3 | 1 | 1 | 1 | **36** | -15 | -4 | -2 | 2 | 4 | -6 | -18 | -6 | -4 | -2 | -17 | -15 | -14 | **35** |
| 15 | Andiappan | 58/M | N | N | Y | - | AW | Y | S | 1 | 2 | 3 | 3 | 2 | 1 | 1 | 2 | 3 | 3 | 1 | 1 | 1 | **38** | -17 | -6 | -4 | -2 | -4 | -6 | -16 | -11 | -6 | -4 | -18 | -16 | -16 | **37** |
| 16 | Nemelian | 45/M | N | N | Y | - | AW | Y | F | 1 | 2 | 3 | 3 | 2 | 1 | 1 | 2 | 3 | 3 | 1 | 1 | 1 | **24** | -12 | -5 | -4 | 2 | -2 | -12 | -15 | -10 | -2 | 2 | -19 | -17 | -16 | **15** |
| 17 | Krishnan | 54/M | N | Y | Y | F/H | AW | Y | S | 1 | 1 | 2 | 2 | 2 | 1 | 1 | 1 | 2 | 2 | 1 | 1 | 1 | **50** | -20 | -19 | -6 | -8 | -4 | -10 | -21 | -10 | 2 | -6 | -21 | -20 | -16 | **45** |
| 18 | Muthiah | 68/M | Y | Y | N | - | AW | Y | F | 1 | 2 | 2 | 2 | 2 | 2 | 1 | 2 | 2 | 2 | 1 | 1 | 1 | **38** | -12 | -2 | 2 | 4 | -8 | -4 | -15 | -10 | -4 | 0 | -18 | -16 | -17 | **26** |
| 19 | Chinnakaruppu | 44/M | N | N | Y | - | AW | Y | F | 2 | 3 | 3 | 3 | 3 | 3 | 2 | 2 | 2 | 2 | 1 | 1 | 1 | **22** | -10 | -5 | 4 | 2 | -6 | -4 | -8 | -14 | -10 | 4 | -18 | -19 | -16 | **15** |
| 20 | Packiam | 39/F | Y | Y | N | - | AW | Y | S | 1 | 2 | 2 | 2 | 2 | 1 | 1 | 2 | 2 | 2 | 1 | 1 | 1 | **40** | -16 | -10 | 3 | 4 | -5 | -12 | -16 | 2 | 0 | 5 | -20 | -16 | -19 | **32** |
| 21 | John Clement | 48/M | N | N | Y | F/H | AW | Y | S | 2 | 2 | 3 | 3 | 2 | 1 | 1 | 1 | 2 | 2 | 1 | 1 | 1 | **41** | -23 | -8 | -11 | 4 | 5 | -11 | -22 | -14 | -9 | -2 | -20 | -20 | -17 | **38** |
| 22 | Karuppiah | 55/M | N | N | Y | - | AW | Y | F | 2 | 3 | 3 | 3 | 3 | 2 | 1 | 2 | 3 | 3 | 1 | 1 | 1 | **25** | -10 | -2 | -4 | 1 | -5 | -10 | -11 | -6 | 0 | 4 | -14 | -12 | -15 | **22** |
| 23 | Subramanian | 61/M | N | N | Y | - | AW | Y | S | 1 | 1 | 2 | 2 | 1 | 1 | 1 | 1 | 2 | 2 | 1 | 1 | 1 | **36** | -17 | -11 | -6 | -8 | -16 | -17 | -21 | -20 | 2 | -4 | -22 | -16 | -19 | **34** |
| 24 | Chandran | 70/M | Y | Y | N | - | AW | N | - | 1 | 2 | 2 | 2 | 2 | 2 | 2 | 2 | 2 | 2 | 1 | 1 | 1 | **35** | -14 | -5 | 0 | 3 | -6 | -5 | -11 | -4 | -10 | -6 | -18 | -17 | -17 | **32** |
| 25 | Vasantha | 58/F | N | N | N | - | AW | Y | S | 1 | 2 | 2 | 3 | 2 | 1 | 1 | 2 | 3 | 3 | 1 | 1 | 1 | **40** | -20 | -4 | -2 | 2 | -7 | -18 | -20 | -10 | -5 | -8 | -22 | -21 | -18 | **38** |
| 26 | Boopalan | 54/M | N | Y | Y | F/H | AW | Y | S | 1 | 3 | 2 | 2 | 2 | 2 | 2 | 1 | 2 | 2 | 1 | 1 | 1 | **41** | -22 | -15 | -2 | 3 | -4 | -6 | -7 | -21 | -11 | -9 | -21 | -20 | -14 | **45** |
| 27 | NoorMohd. | 63/M | N | Y | N | - | AW | N | - | 1 | 2 | 2 | 2 | 2 | 2 | 1 | 1 | 2 | 2 | 1 | 1 | 1 | **44** | -20 | -10 | -4 | 1 | -2 | -15 | -17 | -14 | -8 | -7 | -16 | -15 | -17 | **41** |
| 28 | Meerabai | 65/F | N | N | N | - | AW | Y | S | 2 | 3 | 3 | 3 | 2 | 1 | 2 | 1 | 3 | 3 | 1 | 1 | 1 | **33** | -19 | -7 | -4 | -3 | -9 | -17 | -19 | -12 | -5 | -6 | -18 | -23 | -19 | **35** |
| 29 | Chellam | 34/M | Y | Y | N | HC | AW | N | - | 1 | 2 | 3 | 2 | 2 | 1 | 3 | 2 | 3 | 3 | 1 | 1 | 1 | **39** | -13 | -3 | 2 | 1 | -7 | -13 | -15 | -2 | 2 | -1 | -23 | -19 | -21 | **34** |
| 30 | Ayyavoo | 60/M | N | N | Y | - | AW | Y | F | 2 | 2 | 3 | 3 | 1 | 2 | 2 | 1 | 3 | 3 | 1 | 1 | 1 | **31** | -13 | -4 | -4 | -1 | -7 | -9 | -11 | -3 | -6 | 2 | -13 | -15 | -19 | **27** |
| 31 | Poomayil | 55/F | Y | N | N | - | AW | Y | S | 1 | 3 | 2 | 2 | 1 | 1 | 2 | 1 | 2 | 1 | 1 | 1 | 1 | **44** | -17 | -5 | 1 | -9 | -8 | -5 | -13 | -9 | -10 | -4 | -18 | -21 | -16 | **39** |
| 32 | Rajapandi | 42/M | N | N | Y | F/H | AW | Y | S | 1 | 2 | 2 | 2 | 1 | 2 | 2 | 1 | 2 | 2 | 1 | 1 | 1 | **47** | -21 | -9 | -6 | 1 | -11 | -13 | -18 | -14 | -5 | -7 | -21 | -19 | -17 | **48** |

## TABLE FOR INFERIOR WALL MI

| | | | | | | | | | | WALL MOTION SCORE INDEX | | | | | | | | | | | | | | PEAK SYSTOLIC LONGITUDINAL STRAIN | | | | | | | | | | | | |
|---|---|---|---|---|---|---|---|---|---|---|---|---|---|---|---|---|---|---|---|---|---|---|---|---|---|---|---|---|---|---|---|---|---|---|---|---|
| S.No | Name | Age/Sex | DM | SHT | Smokir | Other | MI | SK | Resul | BS | MS | ApS | Apex | ApL | ML | BL | BA | MA | ApA | BI | MI | ApI | F(2D | BS | MS | ApS | Apex | ApL | ML | BL | BA | MA | ApA | BI | MI | ApI | oy Strain |
| 1 | Karuppasamy | 48/M | N | N | Y | - | IW | Y | S | 1 | 1 | 1 | 1 | 1 | 1 | 1 | 1 | 1 | 1 | 2 | 2 | 2 | 46 | -29 | -26 | -20 | -16 | -8 | -14 | -22 | -20 | -19 | -15 | -4 | 2 | -6 | 40 |
| 2 | Periyalaruppan | 60/M | Y | Y | Y | HC | IW | Y | S | 2 | 1 | 1 | 1 | 1 | 1 | 2 | 1 | 1 | 1 | 3 | 3 | 3 | 40 | 4 | -14 | -12 | -12 | -10 | -6 | -11 | -19 | -17 | -19 | -6 | -2 | 4 | 42 |
| 3 | Soliappan | 44/M | N | N | Y | - | IW | Y | S | 2 | 1 | 1 | 1 | 2 | 2 | 2 | 1 | 1 | 1 | 2 | 2 | 2 | 42 | -11 | -12 | -7 | -10 | -8 | -6 | -13 | -16 | -19 | -14 | -11 | 8 | -5 | 36 |
| 4 | Shanmurarajan | 55/M | N | N | Y | - | IW | N | - | 2 | 1 | 1 | 1 | 1 | 1 | 1 | 1 | 1 | 1 | 2 | 2 | 2 | 49 | -9 | -16 | -15 | -12 | -6 | -18 | -17 | -20 | -21 | -18 | -5 | -11 | 2 | 45 |
| 5 | Kalamegam | 42/M | N | N | Y | - | IW | Y | S | 2 | 1 | 1 | 1 | 1 | 1 | 1 | 1 | 1 | 1 | 3 | 3 | 3 | 45 | -12 | -18 | -19 | -14 | -20 | -18 | -19 | -21 | -17 | -18 | -6 | -4 | 4 | 51 |
| 6 | Jegadeeasan | 68/M | Y | N | N | - | IW | Y | S | 3 | 2 | 1 | 1 | 2 | 2 | 1 | 1 | 1 | 1 | 2 | 2 | 2 | 35 | -2 | -16 | -15 | -20 | -11 | -10 | -22 | -24 | -19 | -19 | -7 | -2 | -9 | 40 |
| 7 | Sivagami | 58/F | Y | Y | N | - | IW | Y | S | 2 | 1 | 1 | 1 | 2 | 1 | 1 | 1 | 1 | 1 | 3 | 3 | 3 | 50 | 4 | -21 | -16 | -16 | -15 | -21 | -17 | -22 | -18 | -17 | -14 | 6 | 4 | 48 |
| 8 | Indrani | 49/F | N | N | N | - | IW | Y | S | 2 | 1 | 1 | 1 | 1 | 1 | 1 | 1 | 1 | 1 | 2 | 2 | 2 | 45 | -5 | -17 | -18 | -17 | -17 | -14 | -19 | -24 | -18 | -19 | 6 | -7 | -7 | 53 |
| 9 | Anandan | 52/M | N | N | Y | - | IW | N | _ | 2 | 1 | 1 | 1 | 1 | 1 | 1 | 1 | 1 | 1 | 2 | 2 | 2 | 54 | -14 | -16 | -17 | -15 | -14 | -12 | -11 | -22 | -18 | -17 | -10 | -1 | -6 | 51 |
| 10 | Meena | 45/F | Y | N | N | - | IW | Y | S | 2 | 2 | 1 | 1 | 2 | 2 | 1 | 1 | 1 | 1 | 3 | 2 | 2 | 40 | -10 | -17 | -18 | -17 | -11 | -8 | -10 | -18 | -17 | -17 | -4 | -10 | -4 | 44 |
| 11 | Pandi | 65/M | N | Y | Y | - | IW | Y | S | 2 | 1 | 1 | 1 | 1 | 1 | 1 | 1 | 1 | 1 | 3 | 2 | 2 | 52 | -4 | -20 | -16 | -18 | -19 | -19 | -18 | -20 | -19 | -19 | -12 | -4 | -6 | 46 |

| | | | | | | | | | | | | | | | | | | | | | | | | | | | | | | | | | | | |
|---|---|---|---|---|---|---|---|---|---|---|---|---|---|---|---|---|---|---|---|---|---|---|---|---|---|---|---|---|---|---|---|---|---|---|---|
| 12 | Ganesan | 55/M | N | N | Y | - | IW | Y | S | 2 | 1 | 1 | 1 | 2 | 2 | 2 | 1 | 1 | 1 | 3 | 2 | 2 | 42 | -10 | -18 | -17 | -11 | -8 | -8 | -14 | -19 | -19 | -15 | -7 | -5 | 5 | 35 |
| 13 | Baskaran | 34/M | N | N | Y | - | IW | Y | S | 1 | 1 | 1 | 1 | 1 | 1 | 1 | 1 | 1 | 1 | 2 | 2 | 2 | 45 | -27 | -28 | -24 | -18 | -10 | -8 | -23 | -19 | -19 | -18 | -2 | 4 | -4 | 58 |
| 14 | Tirupathi | 48/M | Y | N | N | - | IW | Y | S | 1 | 2 | 1 | 1 | 2 | 2 | 1 | 1 | 1 | 1 | 2 | 3 | 2 | 41 | -3 | -11 | -16 | -19 | -9 | -10 | -21 | -23 | -17 | -21 | -9 | -3 | -10 | 44 |
| 15 | Murugesan | 38/M | N | N | Y | - | IW | Y | S | 2 | 2 | 1 | 1 | 1 | 2 | 2 | 1 | 1 | 1 | 3 | 2 | 3 | 47 | -13 | -12 | -8 | -11 | -7 | -8 | -15 | -17 | -18 | -16 | -13 | 4 | -5 | 41 |
| 16 | Raja | 44/M | N | N | Y | - | IW | N | - | 2 | 2 | 1 | 1 | 2 | 2 | 1 | 1 | 1 | 1 | 2 | 3 | 2 | 39 | -11 | -14 | -12 | -15 | -9 | -18 | -21 | -16 | -21 | -17 | -6 | -11 | 2 | 36 |
| 17 | Ganga | 55/F | N | N | N | - | IW | Y | S | 1 | 2 | 1 | 1 | 2 | 1 | 1 | 1 | 1 | 1 | 3 | 2 | 2 | 48 | -6 | -16 | -9 | -21 | -17 | -12 | -18 | -23 | -19 | -18 | -11 | -7 | -8 | 43 |
| 18 | Rajendran | 50/M | N | N | Y | - | IW | Y | S | 2 | 1 | 1 | 1 | 1 | 2 | 1 | 1 | 1 | 1 | 2 | 3 | 2 | 51 | -26 | -23 | -19 | -17 | -11 | -13 | -19 | -22 | -16 | -15 | -8 | 4 | -5 | 46 |
| 19 | Balu | 62/M | Y | Y | Y | _ | IW | Y | S | 2 | 2 | 1 | 1 | 2 | 1 | 2 | 1 | 1 | 1 | 3 | 2 | 3 | 45 | -9 | -15 | -11 | -14 | -7 | -8 | -13 | -18 | -17 | -21 | -7 | -2 | -6 | 47 |
| 20 | Selvaraj | 42/M | N | N | Y | - | IW | Y | S | 1 | 1 | 1 | 1 | 1 | 2 | 1 | 1 | 1 | 1 | 2 | 3 | 3 | 41 | -12 | -16 | -13 | -11 | -15 | -17 | -21 | -17 | -16 | -19 | -7 | 4 | -5 | 39 |

| Segments | Normal Strain | Wall Motion score index | |
|---|---|---|---|
| BS | 12to24 | 1 | Normal |
| MS | 12to24 | 2 | Hypokinesia |
| ApS | 13to25 | 3 | AkinesiA |
| Ap | 12to22 | 4 | Dyskinesia |
| ApL | 12to22 | 5 | Aneurysm |
| ML | 12to23 | | |
| BL | 12to24 | | |
| BA | 15to29 | | |
| MA | 12to22 | | |
| ApA | 8to18 | | |
| BI | 9to19 | | |
| MI | 9to19 | | |
| ApI | 18to28 | | |

| EF- Ejection Fraction | |
|---|---|
| Normal | >55% |
| Mild LV Dysfunction | 45to54 |
| Moderate LV Dysf | 35to44 |
| Severe Dysfunction | <34% |

| | |
|---|---|
| BS | Basal Septum |
| MS | Mid Septum |
| ApS | Apical Septum |
| ApS | Apex |
| ApL | Apical Lateral |
| ML | Mid Lateral |
| BL | Basal Lateral |
| BA | Basal Anterior |
| MA | Mid Anterior |
| ApA | Apical Anterior |
| BI | Basal Inferior |
| MI | Mid Inferior |
| ApI | Apical Inferior |

| | |
|---|---|
| DM | Diabetes Mellitus |
| SHT | Systemic Hypertension |
| HC | Hypercholestrolemia |
| MI | Myocardial Infarction |
| SK | Streptokinase |
| F/H | Family History |


PHILIPS iE 33 System